



ELSEVIER

International Journal of Solids and Structures 41 (2004) 5185–5208

INTERNATIONAL JOURNAL OF
SOLIDS and
STRUCTURES

www.elsevier.com/locate/ijsolstr

Analysis of laminated piezoelectric circular cylinders under axisymmetric mechanical and electrical loads with a semi-analytic finite element method

E. Taciroglu ^{a,*}, C.W. Liu ^a, S.B. Dong ^a, C.K. Chun ^b

^a Department of Civil and Environmental Engineering, University of California, 5731E Boelter Hall, Box 951593, Los Angeles 90094, USA

^b Division of Mechanical and Control Engineering, Sun Moon University, Choong Nam 336-708, South Korea

Received 9 October 2003; received in revised form 31 March 2004

Available online 6 May 2004

Abstract

A semi-analytical finite element method is presented for analyzing the behavior of a laminated circular piezoelectric cylinder under axisymmetric mechanical and electric loads. In this computationally efficient method, discretization occurs in the thickness direction so that any number of layers with distinct material properties and thicknesses can be accommodated. One end of this cylinder is assumed to be clamped and the other end is free. The mechanical loads include axial force, torque, any distribution of pressure, longitudinal and circumferential surface shears, as long as they can be represented by a power series in the axial coordinate. Electric loadings include voltage differences through the thicknesses as well as voltage or surface charge distributions along the axis of the cylinder. Herein, loading conditions leading to uniform, linearly and quadratically varying stress and electric displacement fields are considered. From the discussion of these cases, the extension of the method to higher order axial variations of the loads will be apparent. This problem and its solution procedure can be considered as an extension of Saint-Venant and Almansi-Michell problems for elastic bodies to piezoelectric bodies. A number of verification examples are given where it can be seen that the present results compare extremely well with known analytical solutions for a homogeneous cylinder and with numerical results obtained via three-dimensional finite element analyses. In addition, an example problem on actuation and sensing is provided to demonstrate the utility of the present technique for evaluating designs of this type of smart structures.

© 2004 Elsevier Ltd. All rights reserved.

Keywords: Piezoelectricity; Semi-analytic methods; Smart structures; Sensors; Actuators

*Corresponding author. Tel.: +1-310-2674655; fax: +1-310-2062222.

E-mail address: etacir@seas.ucla.edu (E. Taciroglu).

1. Introduction

Many applications have exploited the piezoelectric effect, including those in the fields of communications, hydro-acoustics, electro-optics and transducer technologies. Much of this technology is well known and familiar, and dwelling further on the virtues of the piezoelectric coupling phenomenon is not necessary. More recently, there has been an upsurge of activity in the development of smart or adaptive structures, wherein these materials provide the means for sensing and actuation in passive and active control of structural behavior. This paper is devoted to the quasi-static analysis of a circular piezoelectric cylinder under general axisymmetric mechanical and electrical loads. The method of analysis described here provides solutions so that the coupled behavior can be clearly evaluated. An enlightened understanding of the piezoelectric coupling behavior in such cylinders will enable designs that can enhance their sensing and actuation functions.

The circular cylinder under consideration may be composed of any number of perfectly bonded layers, each of a uniform thickness with distinct cylindrical piezoelectric properties. The analysis is based on linear three-dimensional theory and semi-analytical finite elements where the discretization occurs over the thickness of the cylinder. The formulation leads to a system of second-order ordinary differential equations governing the nodal variables of the finite element model. While the axisymmetric loading may be general along the length of the cylinder, its representation must be in polynomial form of the axial coordinate z . The stress and electric displacement states resulting from these load components will in turn exhibit behaviors of polynomial form, beginning with the axially uniform state, followed by states that vary linearly, quadratically, etc. The general analysis scheme is first set forth. This is followed by detailed studies of the first three polynomial terms of the axisymmetric load representation. In each case, the displacement and potential fields in the axial direction is postulated at the outset, but the thickness distribution is left unspecified. Based on this representation of the fields, a planar problem for the behavior in a generic cross-section can be posed whose solution defines the functional form of the displacement field and voltage over the thickness of the cylinder. Then, by imposing end conditions, lateral surface electric conditions, and global equilibrium, it is possible to determine the generalized coordinates which are the amplitudes of the displacement and the electric (potential) fields. From the discussion of these three load terms, the solution form for the higher order polynomial loading terms will be apparent. The problem statement and solution technique is an extension of the relaxed formulation of the Saint-Venant and Almansi-Michell problems for prismatic elastic cylinders. Within the framework of this type of analysis, end tractions cannot be prescribed on a point-wise basis but must be given in terms of integrals of these tractions.

A review of literature on the analysis of prismatic piezoelectric structures under quasi-static mechanical and electrical loads from the viewpoint of the Saint-Venant and Almansi-Michell problems shows the papers of Iesan (1987), Batra and Yang (1995), Davi (1996), Bisegna (1998), Ma et al. (2001), Tarn (2002) and Galic and Horgan (2002, 2003) to be relevant. Those of Ma et al. (2001), Tarn (2002) and Galic and Horgan (2002, 2003), are especially pertinent as they consider circular piezoelectric cylinders under generalized plane strain conditions. Validation of the computer code, developed for determining numerical results with the semi-analytical method, was achieved through comparisons with analytical results of these authors as well as those obtained through a proprietary finite element analysis package (ANSYS, 1998). The analytical and numerical methods for circular piezoelectric cylinders had their antecedence in purely mechanical problems involving circular anisotropic cylinders. Many references on such problems are cited by Ma et al. (2001) and Tarn (2002) (viz., Ting, 1996, 1999). In this respect, the numerical analysis procedure presented here is an extension of that developed by Huang and Dong (2001) for laminated, anisotropic, circular cylinders.

In the following two sections, we set forth the governing equations and general solution strategy. Then, the problems of mechanical and electrical loadings leading to axially uniform, linear, and quadratic stress states are considered together with examples. Lastly, some concluding remarks are provided.

2. Summary of governing equations

Consider a laminated piezoelectric cylinder of length L as shown in Fig. 1, where one end is restrained and the other end is free (clamped end is at $z = L$ and the tip is at $z = 0$). The thickness profile may consist of any number of perfectly bonded layers, each possessing distinct thickness and linear piezoelectric properties. We adopt cylindrical coordinates (r, θ, z) with the origin located at the center on the tip end cross-section and the z -axis running toward the clamped end.

The primary dependent variables are the components of the mechanical displacement $\mathbf{u} = [u, v, w]^T$, stress $\boldsymbol{\sigma} = [\sigma_{rr}, \sigma_{\theta\theta}, \sigma_{zz}, \sigma_{\theta z}, \sigma_{rz}, \sigma_{r\theta}]^T$, strain $\boldsymbol{\varepsilon} = [\varepsilon_{rr}, \varepsilon_{\theta\theta}, \varepsilon_{zz}, \varepsilon_{\theta z}, \varepsilon_{rz}, \varepsilon_{r\theta}]^T$, electric displacement $\mathbf{D} = [D_r, D_\theta, D_z]^T$ and electric field $\mathbf{E} = [E_r, E_\theta, E_z]^T$. It is convenient in our solution procedure to concatenate the mechanical and electrical variables as

$$\mathbf{q} = \begin{Bmatrix} \boldsymbol{\varepsilon} \\ \mathbf{E} \end{Bmatrix}_{9 \times 1}, \quad \mathbf{Q} = \begin{Bmatrix} \boldsymbol{\sigma} \\ \mathbf{D} \end{Bmatrix}_{9 \times 1}, \quad \mathbf{v} = \begin{Bmatrix} \mathbf{u} \\ \phi \end{Bmatrix}. \quad (1)$$

For a given laminate of the piezoelectric cylinder, the constitutive relation is

$$\mathbf{Q} = \mathbf{C}^* \mathbf{q}, \quad \text{where} \quad \mathbf{C}^* = \begin{bmatrix} \mathbf{c} & -\mathbf{e} \\ \mathbf{e}^T & \epsilon \end{bmatrix}. \quad (2)$$

In addition, there are generalized strain-displacement relations of the form

$$\mathbf{q} = \mathcal{L}\{\mathbf{v}\} = \left[\frac{1}{2} (\nabla \mathbf{u} + \nabla^T \mathbf{u}), -\nabla \phi \right]^T \quad (3)$$

where ϕ is the electric potential (voltage). The governing equations are based on a semi-analytical finite element formulation, where the discretization occurs in the thickness direction of the cylinder by constant thickness layers, each capable of enjoying distinct piezoelectric properties and thickness. This method of formulation was used by Siao et al. (1994), who derived discrete equations of motion for the study of mechanical vibrations and waves in circular piezoelectric cylinders. Here, the elastostatic form of these equations are used. Since much of the details of such a semi-analytical finite element formulation are given in Siao et al. (1994), only the essence of the method is provided here.

In this version of the semi-analytical finite element formulation, the dependencies in the axial and circumferential directions is left undetermined at the outset, but finite element modeling is used for the radial behavior in the form of three-node cylindrical laminas with quadratic interpolations. This kinematic field on the element level is written as

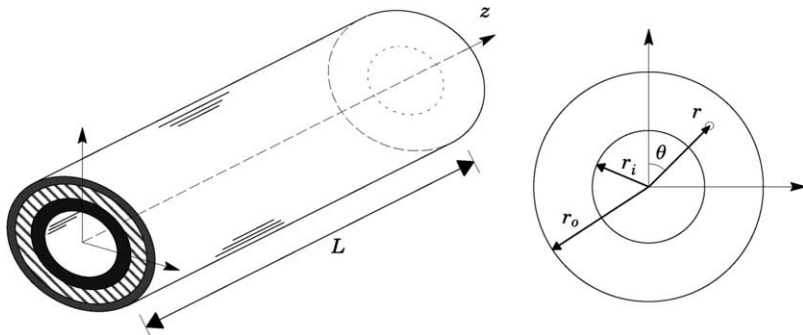


Fig. 1. Problem geometry and the coordinate system.

$$\begin{Bmatrix} u(r, \theta, z) \\ v(r, \theta, z) \\ w(r, \theta, z) \\ \phi(r, \theta, z) \end{Bmatrix} = \begin{bmatrix} \mathbf{n}(r) & \cdot & \cdot & \cdot \\ \cdot & \mathbf{n}(r) & \cdot & \cdot \\ \cdot & \cdot & \mathbf{n}(r) & \cdot \\ \cdot & \cdot & \cdot & \mathbf{n}(r) \end{bmatrix} \begin{Bmatrix} \mathbf{u}(\theta, z) \\ \mathbf{v}(\theta, z) \\ \mathbf{w}(\theta, z) \\ \phi(\theta, z) \end{Bmatrix} \quad (4)$$

where $(\mathbf{u}, \mathbf{v}, \mathbf{w}, \phi)$ are arrays of the four nodal values of the displacement and electric potential fields for a given element. According to this strategy, the operator \mathcal{L} in Eq. (3) should be partitioned into sub-operators with differentiations with respect to r, θ, z . To wit,

$$\mathcal{L}\{\mathbf{v}\} = [\mathcal{L}_r + \mathcal{L}_\theta + \mathcal{L}_z]\{\mathbf{v}\} \quad (5)$$

Substitution of Eq. (4) into Eq. (5) gives

$$\mathbf{q} = \mathbf{b}_1 \mathbf{v} + \mathbf{b}_2 \mathbf{v}_\theta + \mathbf{b}_3 \mathbf{v}_z \quad (6)$$

where $(\mathbf{b}_1, \mathbf{b}_2, \mathbf{b}_3)$ are strain-transformation matrices. Hence the element kinetic quantities are

$$\mathbf{Q} = \mathbf{C}^* [\mathbf{b}_1 \mathbf{v} + \mathbf{b}_2 \mathbf{v}_\theta + \mathbf{b}_3 \mathbf{v}_z]. \quad (7)$$

The theorem of minimum potential energy, where an electric enthalpy function due to Tiersten (1969) serves as the Lagrangian integrand, is used to derive the governing kinematic equations of equilibrium in the form

$$\mathbf{K}_1 \mathbf{V} + \mathbf{K}_2 \mathbf{V}_{,\theta} + \mathbf{K}_3 \mathbf{V}_{,z} - \mathbf{K}_4 \mathbf{V}_{,\theta\theta} - \mathbf{K}_5 \mathbf{V}_{,\theta z} - \mathbf{K}_6 \mathbf{V}_{,zz} = \mathbf{F}(\theta, z) \quad (8)$$

where $\mathbf{F}(\theta, z)$ is the assembled consistent load vector for applied surface tractions, electrical inputs, and the body forces; and $\mathbf{V}(\theta, z)$ is the assembled array of nodal displacements and electric potentials

$$\mathbf{V}(\theta, z) = [U, V, W, \phi]^T. \quad (9)$$

The details of the stiffness matrices in Eq. (8) may be found in Siao et al. (1994), where it was shown that \mathbf{K}_1 , \mathbf{K}_4 , \mathbf{K}_5 , and \mathbf{K}_6 are symmetric, while \mathbf{K}_2 , and \mathbf{K}_3 are antisymmetric. For a finite element model consisting of N nodes, each component, U, V, W or ϕ in \mathbf{V} is N -dimensional, so that each stiffness matrix \mathbf{K}_i will be of size $(4N \times 4N)$.

Herein, we are concerned with loading conditions on the cylinder by tractions and electrical loadings on its lateral surfaces, and by body forces that are axisymmetric only, so that $\mathbf{V} = \mathbf{V}(z)$ and Eq. (8) reduces to

$$\mathbf{K}_1 \mathbf{V} + \mathbf{K}_3 \mathbf{V}_{,z} - \mathbf{K}_6 \mathbf{V}_{,zz} = \mathbf{F}(z). \quad (10)$$

3. General solution strategy

In our analysis procedure, the axisymmetric load $\mathbf{F}(z)$ must be expressed as polynomials of z . To wit

$$\mathbf{F}(z) = \mathbf{F}_0 + z \mathbf{F}_1 + z^2 \mathbf{F}_2 + \cdots + z^k \mathbf{F}_k + \cdots + \mathbf{F}_{0c}(z) + \mathbf{F}_{1c}(z) + \mathbf{F}_{2c}(z) + \cdots + \mathbf{F}_{kc}(z) + \cdots \quad (11)$$

On the tip end, axial and torsional shear tractions may occur. Electrical inputs may be imposed on both the tip and root ends. Each polynomial term \mathbf{F}_k pertaining to the mechanical loads and body forces in Eq. (11) can be separated into two parts

$$\mathbf{F}_k = \mathbf{F}_{ka} + \mathbf{F}_{kb} \quad (k = 0, 1, 2, \dots), \quad (12)$$

where \mathbf{F}_{ka} accounts for these loads which are void of any resultant force or moment in the z -direction, while \mathbf{F}_{kb} allows for such resultants. Examples of \mathbf{F}_{0a} are uniform external and internal pressures, and centrifugal forces ($\omega^2 r$ loads), \mathbf{F}_{1a} contains the nodal values of linear variations of these loads. Examples of \mathbf{F}_{0b} are uniform axial and circumferential surface shear tractions and axial body force, and \mathbf{F}_{1b} represents the linear

variations of them. In addition, Each polynomial term $\mathbf{F}_{jc}(z)$ pertaining to the electric loads can be written as

$$\mathbf{F}_{jc}(z) = \mathbf{F}_{jc0} + z\mathbf{F}_{jc1} + z^2\mathbf{F}_{jc2} + \cdots + z^j\mathbf{F}_{jcj}. \quad (13)$$

Load vectors \mathbf{F}_{jc0} are intended for a potential difference between the inner and outer lateral surfaces that is uniform in z , \mathbf{F}_{jc1} for linear variations of this potential differences, \mathbf{F}_{jc2} for quadratic variations, etc. In general, these forces are not known a priori as their values arise not only from direct electric input, but also from the mechanical behavior through piezoelectric coupling.

The solution to Eq. (10) with loads in the form of Eq. (11) can be stated in series form as

$$\mathbf{V}(z) = \mathbf{V}_0(z) + \mathbf{V}_1(z) + \cdots + \mathbf{V}_k(z) + \cdots, \quad (14)$$

where each component $\mathbf{V}_k(z)$ represents a particular axial variation of the piezoelectric state, i.e., $\mathbf{V}_0(z)$ represents a uniform state, $\mathbf{V}_1(z)$ a linear state, etc. Substituting Eqs. (11) and (14) into Eq. (10) yields an equation, which can be separated into following systems of equations:

$$\mathbf{K}_1\mathbf{V}_0 + \mathbf{K}_3\mathbf{V}_{0,z} - \mathbf{K}_6\mathbf{V}_{0,zz} = \mathbf{F}_{0a} + \mathbf{F}_{0c0}, \quad (0)$$

$$\mathbf{K}_1\mathbf{V}_1 + \mathbf{K}_3\mathbf{V}_{1,z} - \mathbf{K}_6\mathbf{V}_{1,zz} = \mathbf{F}_{0b} + \mathbf{F}_{1c0} + z(\mathbf{F}_{1a} + \mathbf{F}_{1c1}), \quad (1)$$

⋮

$$\mathbf{K}_1\mathbf{V}_k + \mathbf{K}_3\mathbf{V}_{k,z} - \mathbf{K}_6\mathbf{V}_{k,zz} = z^{k-1}\mathbf{F}_{(k-1)b} + z^k\mathbf{F}_{ka} + \mathbf{F}_{kc0} + z\mathbf{F}_{kc1} + \cdots + z^k\mathbf{F}_{kck}. \quad (k)$$

This grouping is predicated on a particular loading condition inducing a corresponding axially varying piezoelectric state. As they shall be referred in the sequel as *Problem I*, *Problem II*, etc., respectively, problem (15.0) involves a uniform stress and electric displacement state in z , problem (15.1) a linear state in z , etc. (see, Fig. 2). The analysis of these equations is pursued by sequentially solving for \mathbf{V}_0 , \mathbf{V}_1 , etc.

Prescribed end conditions must be given for every equation in (15). Since a relaxed formulation is presumed, the end conditions need only to be met on an integral basis in terms of the resultants of tractions and electric displacement. The resultants over a cross-section at any station z along the length of this cylinder are given by the integrals

$$\begin{aligned} P_z(z) &= 2\pi \int_{r_i}^{r_o} \sigma_{zz}(z)r \, dr, & M_z(z) &= 2\pi \int_{r_i}^{r_o} \sigma_{\theta z}(z)r^2 \, dr; \\ \overline{D}_z(z) &= 2\pi \int_{r_i}^{r_o} D_z(z)r \, dr. \end{aligned} \quad (16)$$

If a solution yields end stress distributions σ_{zz} , $\sigma_{\theta z}$ and σ_{rz} and electric displacement D_z that differ from the conditions on a point-wise basis, this difference is a self-equilibrated state whose effect is confined to a

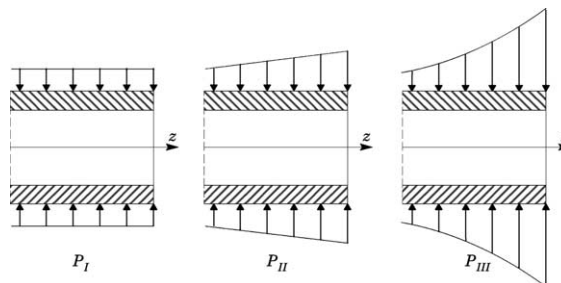


Fig. 2. Sequential problems involving surface tractions and electric loads expressed as polynomials. Problems II and beyond are known as the Almansi-Michell extensions of Saint-Venant's problem.

region near the end according to Saint-Venant's Principle. Means to account for the quantitative manner in which such self-equilibrated states decay into the interior will be addressed in a companion paper.

Global equilibrium must be satisfied by the loads acting on the entire cylinder or on any part of it. These conditions are enforced in the process of the solution. In addition, if there are no electric charges generated or annihilated within the cylinder, then the integral of the outward electric displacement component over the cylinder's entire exterior surface must be zero, i.e.,

$$\int_{\Sigma} \mathbf{D} \cdot \mathbf{n} \, ds = 0, \quad (17)$$

where \mathbf{D} is the electric displacement, \mathbf{n} the unit outward normal to the cylinder, and Σ the exterior surface, which includes the lateral surfaces and the two ends. This conservation requirement is not used in the solution procedure, but it provides an a posteriori consistency check of the results. All of our numerical results will undergo this validation.

4. Solution preliminaries

In the sequential treatment of the series of Eq. (15), the solution vector \mathbf{V}_k at a given step will depend on data from previous steps, i.e., $\mathbf{V}_{k-1}, \mathbf{V}_{k-2}, \dots, \mathbf{V}_0$. According to Ieşan's (1986) method, the appropriate field for a given step is obtained by integrating the solution vector of the previous step once with respect to z . The form of \mathbf{V}_0 —considered in the first step in this procedure—is obtained by integrating rigid body displacements once with respect to z . For axisymmetry, two such rigid body motions are relevant, i.e., axial translation and rotation about the z -axis. Thus, the rigid body motions may be stated as

$$\mathbf{V}_{\text{RB}} = \Phi_{\text{RB}} \mathbf{a}_{\text{RB}}, \quad (18)$$

where \mathbf{a}_{RB} is an array of amplitudes of each rigid body component and Φ_{RB} is a $(4N \times 2)$ matrix of the two rigid body kinematic distributions in r given by

$$\begin{aligned} \mathbf{a}_{\text{RB}} &= [w_0, \omega_z]^T & \text{where} & \quad \begin{cases} \mathbf{R}_3 = [\mathbf{0}, \mathbf{0}, \mathbf{I}, \mathbf{0}]^T \\ \mathbf{R}_6 = [\mathbf{0}, \mathbf{R}, \mathbf{0}, \mathbf{0}]^T \end{cases} \\ \Phi_{\text{RB}} &= [\mathbf{R}_3, \mathbf{R}_6] \end{aligned} \quad (19)$$

with column vectors \mathbf{I} and \mathbf{R} containing N unit entries and the r -coordinates of the N nodes, respectively. Rigid body displacement field \mathbf{V}_{RB} when substituted into the homogeneous form of Eq. (10) gives

$$\mathbf{K}_1 \mathbf{R}_3 = \mathbf{0}, \quad \mathbf{K}_1 \mathbf{R}_6 = \mathbf{0}. \quad (20)$$

On the element level, these rigid body components, denoted by lower case symbols, yield null values when substituted strain-displacement relationships in Eq. (3), i.e.,

$$\mathbf{b}_r \mathbf{r}_3 = \mathbf{0}, \quad \mathbf{b}_r \mathbf{r}_6 = \mathbf{0}. \quad (21)$$

It is noted that there is also a rigid body electrical term in the form of a constant potential in the form

$$\mathbf{V}_{\text{RB}} = \mathbf{R}_7 \mathbf{a}_\phi, \quad \text{where} \quad \mathbf{R}_7 = [\mathbf{0}, \mathbf{0}, \mathbf{0}, \mathbf{I}]^T, \quad (22)$$

which satisfies

$$\mathbf{K}_1 \mathbf{R}_7 = \mathbf{0}. \quad (23)$$

This electrical mode can be added to any solution without affecting any of the stresses or electric displacements. Expressions (20), (21) and (23) are useful identities in our subsequent discussion.

5. Problem I—uniform state

A uniform state is governed by Eq. (15.0); reproduced here as

$$\mathbf{K}_1 \mathbf{V}_0 + \mathbf{K}_3 \mathbf{V}_{0,z} - \mathbf{K}_6 \mathbf{V}_{0,zz} = \mathbf{F}_{0a} + \mathbf{F}_{0c0}. \quad (24)$$

The components of the load vectors on the right-hand side are illustrated in Fig. 3. The mechanical loads must exhibit no resultant axial force or torque. For uniform pressures, say $\bar{\sigma}_{ri}$ and $\bar{\sigma}_{ro}$ on the inner and outer surfaces, r_i and r_o , respectively, their consistent load components are $2\pi r_i \bar{\sigma}_{ri}$ and $-2\pi r_o \bar{\sigma}_{ro}$, and obviously they have no axial resultants. For axial and circumferential surface shear tractions, say $(\bar{\sigma}_{zi}, \bar{\sigma}_{zo})$ and $(\bar{\sigma}_{\theta i}, \bar{\sigma}_{\theta o})$ on the inside and outside surfaces, self-equilibrium of these two traction pairs require that

$$\bar{\sigma}_{zi} 2\pi r_i = \bar{\sigma}_{zo} 2\pi r_o \quad \text{and} \quad \bar{\sigma}_{\theta i} 2\pi r_i^2 = \bar{\sigma}_{\theta o} 2\pi r_o^2. \quad (25)$$

For prescribed inside and outside charges $(\bar{D}_{r_i}, \bar{D}_{r_o})$, the electrical load vector \mathbf{F}_{0c} will have consistent charge terms $(2\pi r_i \bar{D}_{r_i}, 2\pi r_o \bar{D}_{r_o})$. If voltages are prescribed instead, say $\bar{\phi}_i$ and $\bar{\phi}_o$, the resulting solution will yield a distribution of D_r over the thickness. For an admissible electrostatic solution, the total charges over the cylinder's exterior surfaces must be conserved, whether they are prescribed or computed. This conservation principle requires that D_{r_i} and D_{r_o} must obey

$$D_{r_i} 2\pi r_i = D_{r_o} 2\pi r_o. \quad (26)$$

At the tip end $z = 0$, an axial force P_z and torque M_z may be applied. Within the framework of a Saint-Venant solution, the restraint at the clamped end involves some fixity condition. Therefore, the present solution will be unique only within a rigid body displacement.

5.1. Analysis

The most general form of the kinematic field for Eq. (24) is

$$\mathbf{V}_0 = a_{13}(z \mathbf{R}_3 + \Psi_{13}) + a_{16}(z \mathbf{R}_6 + \Psi_{16}) + \mathbf{U}_{IP} + \sum_{x=1} c_{Ix} \mathbf{U}_{IEz} + \Phi_{RB} \mathbf{a}_{RB}. \quad (27)$$

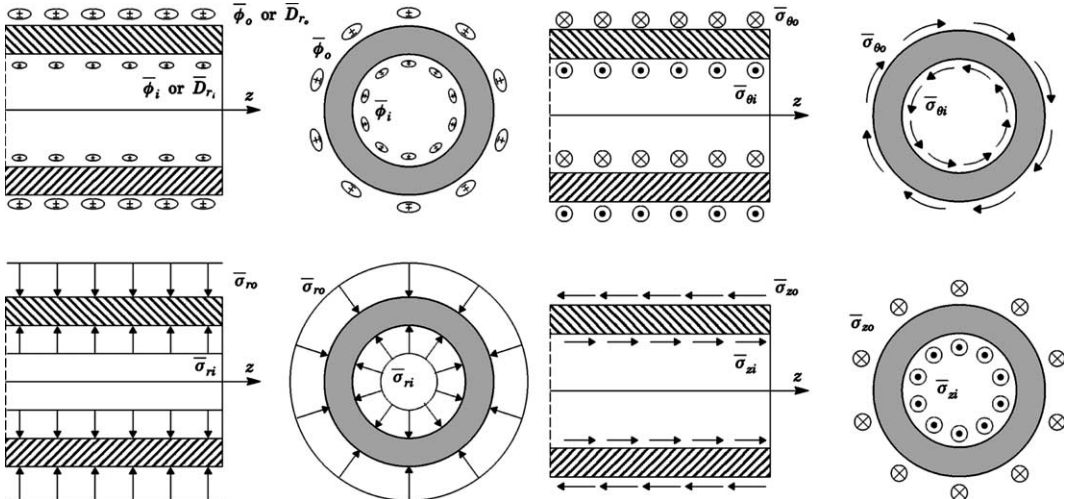


Fig. 3. Surface tractions, electric potential, and electric displacements considered in Problem I. Axial and circumferential surface tractions must be self-equilibrated. This requirement is removed for higher-order problems.

The first two terms with generalized coordinates a_{13} and a_{16} relate to extension and torsion, where $(z\mathbf{R}_3, z\mathbf{R}_6)$ and (Ψ_{13}, Ψ_{16}) represent the primal behavior and cross-sectional warpages, respectively, and \mathbf{U}_{IP} represents the particular solution for mechanical loads \mathbf{F}_{0a} . The series \mathbf{U}_{IEz} with amplitudes c_{1z} represent the response to electric loading \mathbf{F}_{0c} . The number of terms is a function of the number of cylindrical surfaces with prescribed electric conditions. Herein, two will be used, for inside and outside surface electric conditions. Lastly, $\Phi_{RB}\mathbf{a}_{RB}$ is a rigid body displacement whose values depend on the restraint conditions at the root end of the cylinder. This kinematic field can be obtained by integrating rigid body displacement (18) once with respect to z . Substitution of Eq. (27) into Eq. (24) gives

$$z[a_{13}\mathbf{K}_1\mathbf{R}_3 + a_{16}\mathbf{K}_1\mathbf{R}_6] + a_{13}\{\mathbf{K}_1\Psi_3 + \mathbf{K}_3\mathbf{R}_3\} + a_{16}\{\mathbf{K}_1\Psi_6 + \mathbf{K}_3\mathbf{R}_6\} + [\mathbf{K}_1\mathbf{U}_{IP} - \mathbf{F}_{0a}] + \left[\sum_{z=1}^2 \{c_{1z}\mathbf{K}_1\mathbf{U}_{IEz}\} - \mathbf{F}_{0c0} \right] = 0. \quad (28)$$

To satisfy Eq. (28), each square bracketed term must vanish. Those multiplied by z vanish due to the identities presented in Eq. (20). The warpages (Ψ_3, Ψ_6) and the particular solution \mathbf{U}_{IP} are determined by

$$\mathbf{K}_1\Psi_{13} = -\mathbf{K}_3\mathbf{R}_3, \quad \mathbf{K}_1\Psi_{16} = -\mathbf{K}_3\mathbf{R}_6, \quad \mathbf{K}_1\mathbf{U}_{IP} = \mathbf{F}_{0a}. \quad (29)$$

Electric load vector \mathbf{F}_{0c0} is not known a priori, as it depends on the lateral surface electric conditions, which are composed of all terms in \mathbf{V}_0 . Hence, $c_{1z}\mathbf{U}_{IEz}$'s cannot be determined. However, we can let \mathbf{U}_{IEz} be the response to a unit electric charge or flux on a cylindrical surface $r = r_z$. Denoting this load vector by \mathbf{f}_{0cz} , which only contains a unit charge in the appropriate degree of freedom; then \mathbf{U}_{IEz} satisfies

$$\mathbf{K}_1\mathbf{U}_{IEz} = \mathbf{f}_{0cz} \quad (z = 1, 2). \quad (30)$$

To invert Eqs. (29) and (30), kinematic restraints must be imposed to preclude rigid body motions. With respect to the potential ϕ , the problem involves the grounding of a surface. Thus, for a unit outside surface charge, the inside surface is grounded, and for a unit inside surface charge, the outside surface is grounded.

After determining these distributions, the nodal stress and electric displacement distributions \mathbf{Q} can be constructed as

$$\mathbf{Q} = a_{13}\mathbf{C}^*(\mathbf{b}_r\Psi_{13} + \mathbf{b}_z\mathbf{r}_3) + a_{16}\mathbf{C}^*(\mathbf{b}_r\Psi_{16} + \mathbf{b}_z\mathbf{r}_6) + \mathbf{C}^*\mathbf{b}_r\mathbf{U}_{IP} + \mathbf{C}^*\left(\sum_{z=1}^2 c_{1z}\mathbf{b}_r\mathbf{U}_{IEz}\right). \quad (31)$$

The integrals of σ_{zz} and $\sigma_{\theta z}$ over any generic cross-section according to Eq. (16) gives

$$\begin{Bmatrix} P_z \\ M_z \end{Bmatrix} = \begin{bmatrix} \kappa_{133} & \kappa_{136} \\ \kappa_{136} & \kappa_{166} \end{bmatrix} \begin{Bmatrix} a_{13} \\ a_{16} \end{Bmatrix} + \begin{Bmatrix} P_{IP} \\ M_{IP} \end{Bmatrix} + \sum_{z=1}^2 c_{1z} \begin{Bmatrix} P_{IEz} \\ M_{IEz} \end{Bmatrix}, \quad (32)$$

where κ_{1ij} , ($i, j = 3, 6$) are the cross-sectional stiffness influence coefficients given by

$$\begin{aligned} \kappa_{133} &= 2\pi \sum_{m=1}^M \int \sigma_{zz13} r dr, & \kappa_{166} &= 2\pi \sum_{m=1}^M \int \sigma_{\theta z16} r^2 dr \\ \kappa_{136} &= 2\pi \sum_{m=1}^M \int \sigma_{zz16} r dr = 2\pi \sum_{m=1}^M \int \sigma_{\theta z13} r^2 dr \end{aligned} \quad (33)$$

and P_{IP} , M_{IP} , P_{IEz} , and M_{IEz} denote the resultants of the particular solutions for mechanical and electrical loads

$$P_{IP} = 2\pi \sum_{m=1}^M \int \sigma_{zz(IP)} r dr, \quad M_{IP} = 2\pi \sum_{m=1}^M \int \sigma_{\theta z(IP)} r^2 dr, \quad (34)$$

$$P_{IEz} = 2\pi \sum_{m=1}^M \int \sigma_{zz(EIz)} r dr, \quad M_{IEz} = 2\pi \sum_{m=1}^M \int \sigma_{\theta z(EIz)} r^2 dr. \quad (35)$$

Since the stress and electric displacement states are uniform in z , P_z and M_z in Eq.(32) must represent the applied force and torque at the tip end.

Recapitulating, all terms in Eq. (32) are known except for coefficients a_{13} , a_{16} , c_{11} and c_{12} . They are dependent upon the applied force and torque, P_z and M_z and electric surface conditions. A number of electric surface conditions are possible. Four will be considered in the sequel.

5.2. Both surfaces open

In this case, called the *open circuit* condition, there is no specification of lateral surface electric conditions so that there is no need for the terms $c_{1z}U_{IEz}$ in displacement field Eq. (27). Coefficients a_{13} and a_{16} are determined by

$$\begin{bmatrix} \kappa_{133} & \kappa_{136} \\ \kappa_{136} & \kappa_{166} \end{bmatrix} \begin{Bmatrix} a_{13} \\ a_{16} \end{Bmatrix} = \begin{Bmatrix} P_z - P_{IP} \\ M_z - M_{IP} \end{Bmatrix}. \quad (36)$$

5.3. Prescribed voltages on both surfaces

If voltages $(\bar{\phi}_i, \bar{\phi}_o)$, respectively, are prescribed on the inside and outside surfaces, these conditions are given by¹

$$\begin{aligned} \psi_{13\phi}(r_i)a_{13} + \psi_{16\phi}(r_i)a_{16} + U_{IE1\phi}(r_i)c_{11} + U_{IE2\phi}(r_i)c_{12} + U_{IP\phi}(r_i) &= \bar{\phi}_i, \\ \psi_{13\phi}(r_o)a_{13} + \psi_{16\phi}(r_o)a_{16} + U_{IE1\phi}(r_o)c_{11} + U_{IE2\phi}(r_o)c_{12} + U_{IP\phi}(r_o) &= \bar{\phi}_o. \end{aligned} \quad (37)$$

Casting these conditions together with those of Eq. (32) into matrix form yields

$$\begin{bmatrix} \kappa_{133} & \kappa_{136} & P_{IE1} & P_{IE2} \\ \kappa_{136} & \kappa_{166} & M_{IE1} & M_{IE2} \\ \psi_{13\phi}(r_i) & \psi_{16\phi}(r_i) & U_{IE1\phi}(r_i) & U_{IE2\phi}(r_i) \\ \psi_{13\phi}(r_o) & \psi_{16\phi}(r_o) & U_{IE1\phi}(r_o) & U_{IE2\phi}(r_o) \end{bmatrix} \begin{Bmatrix} a_{13} \\ a_{16} \\ c_{11} \\ c_{12} \end{Bmatrix} = \begin{Bmatrix} P_z - P_{IP} \\ M_z - M_{IP} \\ \bar{\phi}_i - U_{IP\phi}(r_i) \\ \bar{\phi}_o - U_{IP\phi}(r_o) \end{Bmatrix}. \quad (38)$$

If $\bar{\phi}_i = \bar{\phi}_o = 0$, the solution for a_{13} , a_{16} , c_{11} and c_{12} define a *short-circuited* condition.

5.4. Prescribed electric displacements

If $\bar{D}_r(r_i)$ and $\bar{D}_r(r_o)$ are prescribed electric charges on the inside and outside surfaces, then

$$\begin{aligned} D_{13r}(r_i)a_{13} + D_{16r}(r_i)a_{16} + D_{IE1r}(r_i)c_{11} + D_{IE2r}(r_i)c_{12} + D_{IPr}(r_i) &= \bar{D}_{r_i}, \\ D_{13r}(r_o)a_{13} + D_{16r}(r_o)a_{16} + D_{IE1r}(r_o)c_{11} + D_{IE2r}(r_o)c_{12} + D_{IPr}(r_o) &= \bar{D}_{r_o}. \end{aligned} \quad (39)$$

The coefficients a_{13} , a_{16} , c_{11} and c_{12} are determined by

$$\begin{bmatrix} \kappa_{133} & \kappa_{136} & P_{IE1} & P_{IE2} \\ \kappa_{136} & \kappa_{166} & M_{IE1} & M_{IE2} \\ D_{13r}(r_i) & D_{16r}(r_i) & D_{IE1r}(r_i) & D_{IE2r}(r_i) \\ D_{13r}(r_o) & D_{16r}(r_o) & D_{IE1r}(r_o) & D_{IE2r}(r_o) \end{bmatrix} \begin{Bmatrix} a_{13} \\ a_{16} \\ c_{11} \\ c_{12} \end{Bmatrix} = \begin{Bmatrix} P_z - P_{IP} \\ M_z - M_{IP} \\ \bar{D}_{r_i} - D_{IPr}(r_i) \\ \bar{D}_{r_o} - D_{IPr}(r_o) \end{Bmatrix}. \quad (40)$$

¹ Subscripts (u, v, w, ϕ) will be used with displacement vectors ψ_{13} , ψ_{16} , U_{IE1} , etc. to designate the corresponding components in these vectors. An expression in parenthesis, for example (r_i) in $\psi_{13\phi}(r_i)$, denotes the nodal location of the given component.

5.5. Mixed electric conditions

Suppose an electric displacement $\bar{D}_r(r_i)$ is prescribed on the inside surface and potential $\bar{\phi}_o$ is given on the outside surface, then equations for the coefficients take the form

$$\begin{bmatrix} \kappa_{133} & \kappa_{136} & P_{IE1} & P_{IE2} \\ \kappa_{136} & \kappa_{166} & M_{IE1} & M_{IE2} \\ D_{13r}(r_i) & D_{16r}(r_i) & D_{IE1r}(r_i) & D_{IE2r}(r_i) \\ \psi_{13\phi}(r_o) & \psi_{16\phi}(r_o) & U_{IE1\phi}(r_o) & U_{IE2\phi}(r_o) \end{bmatrix} \begin{Bmatrix} a_{13} \\ a_{16} \\ c_{11} \\ c_{12} \end{Bmatrix} = \begin{Bmatrix} P_z - P_{IP} \\ M_z - M_{IP} \\ \bar{D}_r - D_{IPr}(r_i) \\ \bar{\phi}_o - U_{IP\phi}(r_o) \end{Bmatrix}. \quad (41)$$

5.6. Validation example for problem I

We shall analyze a homogeneous circular cylinder with a length to thickness ratio $L/t = 20$, and with inner and outer radii to thickness ratios $r_i/t = 1.0$, $r_o/t = 2.0$. The cylinder is made of PZT4 material (lead-zirconium-titanate), which is a widely used piezoceramic in actuator/sensor technology. The material constants for PZT4 are displayed in Table 1 (see, for example, Berlincourt et al., 1964).

The cylinder is subjected to uniform and resultant-free loads. To wit, the applied loads are uniform circumferential shear tractions, $\bar{\sigma}_{\theta i} = 4.0$ Pa, $\bar{\sigma}_{\theta o} = 1.0$ Pa; uniform axial shear tractions, $\bar{\sigma}_{zi} = 2.0$ Pa, $\bar{\sigma}_{zo} = 1.0$ Pa; uniform outside surface voltage $\bar{\phi}_o = 100$ V, and internal pressure $\bar{\sigma}_{ri} = 100$ Pa. The variation of the normalized stresses, displacements and potential through the thickness of the cylinder as computed via the semi-analytic method proposed here and exact solutions by Tarn (2002) are displayed in Fig. 4. The agreement between these two results are remarkable. Furthermore, the total free-surface integral of the normal electric displacements defined in Eq. (17) yield the values of $\{0.0, 1.1 \times 10^{-8}, 6.1 \times 10^{-12}, 0.0\}$ Coulombs for the uniform pressure, uniform potential, self-equilibrated axial and self-equilibrated torsional shear problems, respectively. The corresponding largest individual integrated free-surface fluxes—either of left-face, right-face, interior or exterior surfaces—are $\{3.1 \times 10^{-7}, 2.3 \times 10^{-4}, 1.2 \times 10^{-7}, 0.0\}$ Coulombs, respectively. Noting that the total values (which are ideally equal to zero) are 4–7 orders of magnitude smaller than the individual values. These final results validate the consistency (or of the conservation of electric charges property) of the semi-analytic method.

Also note that the results displayed in Fig. 4 are normalized with respect to their maximum values. These maximum values are omitted for brevity as the validation example is only meant to display the veracity of the semi-analytic approach.

Table 1
Material constants for PZT4 crystal

$c_{11} = 13.90 \times 10^{10}$ (Pa)	$e_{13} = -5.2028$ (C/m ²)	$\epsilon_{11} = 6.4605 \times 10^{-9}$ (F/m)
$c_{33} = 11.54 \times 10^{10}$	$e_{33} = 15.0804$	$\epsilon_{33} = 5.6198 \times 10^{-9}$
$c_{44} = 2.56 \times 10^{10}$	$e_{15} = 12.7179$	$\epsilon_{22} = \epsilon_{11}$
$c_{12} = 7.78 \times 10^{10}$	$e_{23} = e_{13}$	
$c_{13} = 7.43 \times 10^{10}$	$e_{42} = e_{15}$	
$c_{44} = 2.56 \times 10^{10}$		
$c_{66} = 3.06 \times 10^{10}$		
$c_{22} = c_{11}, c_{23} = c_{13}$		
$c_{55} = c_{44}$		

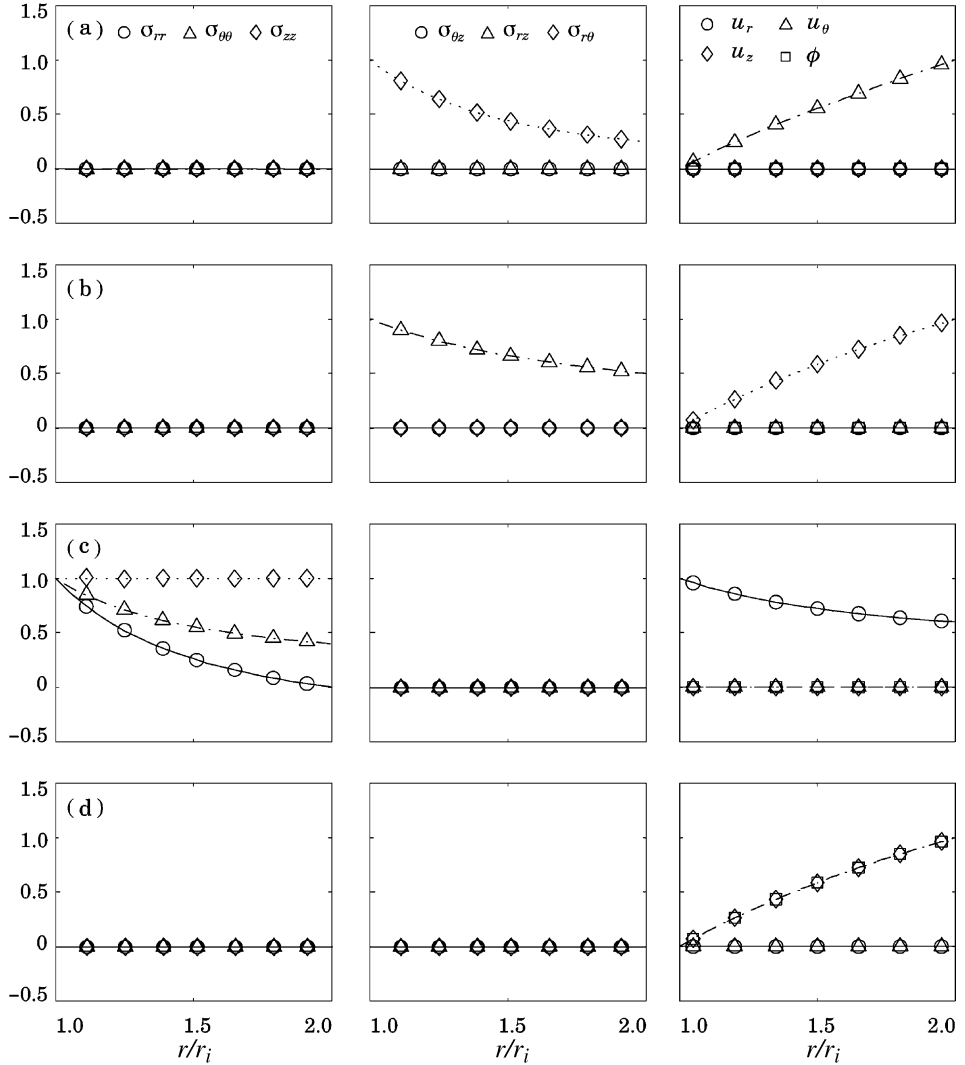


Fig. 4. Validation for Problem I: the results are for self-equilibrated circumferential (Row a) and axial (Row b) shear tractions, and uniform pressure (Row c) and voltage (Row d) distributions prescribed on the exterior surface of the cylinder. The symbols and the (dashed, dotted, etc.) lines denote the semi-analytic and the exact solutions provided by Tarn (2002), respectively.

6. Problem II—linearly varying state

The linearly varying state is governed by Eq. (15.1); reproduced here as

$$\mathbf{K}_1 \mathbf{V}_1 + \mathbf{K}_3 \mathbf{V}_{1,z} - \mathbf{K}_6 \mathbf{V}_{1,zz} = \mathbf{F}_{0b} + \mathbf{F}_{1c0} + z(\mathbf{F}_{1a} + \mathbf{F}_{1c1}). \quad (42)$$

Consistent load vector \mathbf{F}_{1a} represents linearly varying pressure distributions, without an axial resultant, and \mathbf{F}_{0b} represents the uniform axial and circumferential shears with axial force and torque resultants. Uniform and linearly varying electric loads are contained in \mathbf{F}_{1c0} and \mathbf{F}_{1c1} , respectively. Note that a uniform pressure could have been included in \mathbf{F}_{0b} , but pressure as well as self-equilibrated surface axial and circumferential shears were already taken into account in \mathbf{F}_{0a} of Problem I.

6.1. Analysis

The most general form of the displacement field for Eq. (42) is obtained by integrating Eq. (24) once with respect to z , which yields

$$\mathbf{V}_1 = a_{13} \left(\frac{z^2}{2} \mathbf{R}_3 + z \mathbf{\Psi}_{13} + \mathbf{\Psi}_{II3} \right) + a_{16} \left(\frac{z^2}{2} \mathbf{R}_6 + z \mathbf{\Psi}_{16} + \mathbf{\Psi}_{II6} \right) + a_{II3} (z \mathbf{R}_3 + \mathbf{\Psi}_{13}) + a_{II6} (z \mathbf{R}_6 + \mathbf{\Psi}_{16}) + z \mathbf{U}_{IIP1} + \mathbf{U}_{IIP2} + \sum_{\alpha=1}^2 [c_{1\alpha} (z \mathbf{U}_{IE\alpha} + \mathbf{U}_{IIE\alpha}) + c_{II\alpha} \mathbf{U}_{IE\alpha}] + \mathbf{\Phi}_{RB} \mathbf{a}_{RB}, \quad (43)$$

where a_{13} , a_{16} , c_{11} , c_{12} , a_{II3} , a_{II6} , c_{II1} and c_{II2} are the generalized deformation coordinates. In this expression, $\mathbf{\Psi}_{II3}$ and $\mathbf{\Psi}_{II6}$ are new warpages, \mathbf{U}_{IIP1} , \mathbf{U}_{IIP2} are particular solutions for the mechanical loads, and \mathbf{U}_{IIE1} and \mathbf{U}_{IIE2} are new fields for the electric loading. All other vectors are known from previous considerations. Coefficients a_{13} , a_{16} , c_{11} and c_{12} are new and are completely unrelated to the values of Problem I. Note that Eq. (43) can be obtained by integrating Eq. (24) once with respect to z . This method of integrating the previous displacement field for this next level of stress and electric displacement variations follows Ieşan's method (1987) for Saint-Venant's problem.

To determine all of the vectors in Eq. (43), we substitute it into Eq. (42) and this leads to three sets of terms multiplied by z^0 , z^1 and z^2 that contain all of the defining equations. Many of these equations are repetitions of (the rigid body, etc.) identities in Problem I. The new warpages $\mathbf{\Psi}_{II3}$ and $\mathbf{\Psi}_{II6}$ and new particular solutions for the mechanical loads are determined by

$$\mathbf{K}_1 \mathbf{\Psi}_{II3} + \mathbf{K}_3 \mathbf{\Psi}_{13} - \mathbf{K}_6 \mathbf{R}_3 = 0, \quad \mathbf{K}_1 \mathbf{\Psi}_{II6} + \mathbf{K}_3 \mathbf{\Psi}_{16} - \mathbf{K}_6 \mathbf{R}_6 = 0, \quad (44)$$

$$\mathbf{K}_1 \mathbf{U}_{IIP1} - \mathbf{F}_{1a1} = 0, \quad \mathbf{K}_1 \mathbf{U}_{IIP2} + \mathbf{K}_3 \mathbf{U}_{IIP1} - \mathbf{F}_{0b1} = 0. \quad (45)$$

The first of Eq. (45) yields \mathbf{U}_{IIP1} , whereupon the second gives \mathbf{U}_{IIP2} in which the uniform mechanical loads and warpages in $\mathbf{K}_3 \mathbf{U}_{IIP1}$ drive this solution. The equations for the electric terms are

$$\begin{aligned} \sum_{\alpha=1}^2 c_{1\alpha} \mathbf{K}_1 \mathbf{U}_{IE\alpha} &= \mathbf{F}_{1c1}, \\ \sum_{\alpha=1}^2 c_{1\alpha} (\mathbf{K}_1 \mathbf{U}_{IIE\alpha} + \mathbf{K}_3 \mathbf{U}_{IE\alpha}) + \sum_{\alpha=1}^2 c_{II\alpha} \mathbf{K}_1 \mathbf{U}_{IE\alpha} &= \mathbf{F}_{1c0}. \end{aligned} \quad (46)$$

As in Problem I, electric load vector \mathbf{F}_{1c1} depends upon various sources that may not be known at the outset, so that Eq. (46) must be treated in the same way as Problem I. Solutions for $\mathbf{U}_{IE\alpha}$ give the distributions for unit electric charges on the lateral surfaces, and they are identical to those found in Problem I. In the second equation, $\mathbf{U}_{IIE\alpha}$ can be considered to be driven by its corresponding unit solution $\mathbf{U}_{IE\alpha}$, so that the appropriate equation for $\mathbf{U}_{IIE\alpha}$ is

$$\mathbf{K}_1 \mathbf{U}_{IIE\alpha} + \mathbf{K}_3 \mathbf{U}_{IE\alpha} = 0 \quad (\alpha = 1, 2). \quad (47)$$

After the complete displacement field is established, the explicit forms of \mathbf{F}_{1c1} and \mathbf{F}_{1c0} can then be stated, but their forms are not essential (i.e. they are not needed for determining the generalized coordinates).

Upon establishing the displacement field distributions, the (stress and electric displacement) vector \mathbf{Q} within an element can be formed through

$$\begin{aligned}
\mathbf{Q} = & zC^*[a_{13}(\mathbf{b}_r\Psi_{13} + \mathbf{b}_z\mathbf{r}_3) + a_{16}(\mathbf{b}_r\Psi_{16} + \mathbf{b}_z\mathbf{r}_6) + \mathbf{b}_rU_{IIP1}] + C^*[a_{13}(\mathbf{b}_r\Psi_{II3} + \mathbf{b}_z\Psi_{13}) \\
& + a_{16}(\mathbf{b}_r\Psi_{II6} + \mathbf{b}_z\Psi_{16}) + a_{II3}(\mathbf{b}_r\Psi_{13} + \mathbf{b}_z\mathbf{r}_3) + a_{II6}(\mathbf{b}_r\Psi_{16} + \mathbf{b}_z\mathbf{r}_6) + \mathbf{b}_rU_{IIP2} + \mathbf{b}_zU_{IIP1}] \\
& + C^*\sum_{\alpha=1}^2[zc_{I\alpha}\mathbf{b}_r\mathbf{U}_{IE\alpha} + c_{I\alpha}(\mathbf{b}_r\mathbf{U}_{IIE\alpha} + \mathbf{b}_z\mathbf{U}_{IE\alpha}) + c_{II\alpha}\mathbf{b}_r\mathbf{U}_{IE\alpha}].
\end{aligned} \tag{48}$$

Integration of σ_{zz} and $\sigma_{\theta z}$ over a generic cross-section according to Eq. (16) yields

$$\begin{aligned}
\left\{ \begin{array}{l} P_z(z) \\ M_z(z) \end{array} \right\} = & z \left(\begin{bmatrix} \kappa_{133} & \kappa_{136} \\ \kappa_{136} & \kappa_{166} \end{bmatrix} \left\{ \begin{array}{l} a_{13} \\ a_{16} \end{array} \right\} + \left\{ \begin{array}{l} P_{IIP1} \\ M_{IIP1} \end{array} \right\} \right) + \begin{bmatrix} \kappa_{II33} & \kappa_{II36} \\ \kappa_{II36} & \kappa_{II66} \end{bmatrix} \left\{ \begin{array}{l} a_{13} \\ a_{16} \end{array} \right\} + \begin{bmatrix} \kappa_{133} & \kappa_{136} \\ \kappa_{136} & \kappa_{166} \end{bmatrix} \left\{ \begin{array}{l} a_{II3} \\ a_{II6} \end{array} \right\} \\
& + \left\{ \begin{array}{l} P_{IIP2} \\ M_{IIP2} \end{array} \right\} + z \sum_{\alpha} c_{I\alpha} \left\{ \begin{array}{l} P_{IE\alpha} \\ M_{IE\alpha} \end{array} \right\} + \sum_{\alpha} c_{I\alpha} \left\{ \begin{array}{l} P_{IIE\alpha} \\ M_{IIE\alpha} \end{array} \right\} + \sum_{\alpha} c_{II\alpha} \left\{ \begin{array}{l} P_{IE\alpha} \\ M_{IE\alpha} \end{array} \right\},
\end{aligned} \tag{49}$$

where κ_{Iij} 's were defined in Eq. (33) and κ_{IIij} 's have the same formulas as those for κ_{Iij} 's except with σ_{zzII3} and $\sigma_{\theta zII3}$ replacing σ_{zzI3} and $\sigma_{\theta zI3}$, i.e., $\kappa_{II33} = 2\pi \sum_{m=1}^M \int \sigma_{zzII3} r dr$, etc. Similarly, mechanical load resultants (P_{IIPi}, M_{IIPi} , $i = 1, 2$) are given by Eq. (34) except with $\sigma_{zz(IIPi)}$ and $\sigma_{\theta z(IIPi)}$ replacing $\sigma_{zz(IP)}$ and $\sigma_{\theta z(IP)}$, i.e., $P_{IIP1} = 2\pi \sum_{m=1}^M \int \sigma_{zz(IIP1)} r dr$, etc. Electric resultants $P_{IE\alpha}$ and $M_{IE\alpha}$ were defined by Eq. (35) and ($P_{IIE\alpha}, M_{IIE\alpha}$, $\alpha = 1, 2$) are given by the same formula but with $\sigma_{zz(EII\alpha)}$ and $\sigma_{\theta z(EII\alpha)}$ replacing $\sigma_{zz(EI\alpha)}$ and $\sigma_{\theta z(EI\alpha)}$ as in $P_{IIE\alpha} = 2\pi \sum_{m=1}^M \int \sigma_{zz(EII\alpha)} r dr$, etc.

Eq. (49) defines P_z and M_z at any z . They depend on the generalized coordinates, which can be determined in two stages. First, we invoke global equilibrium by requiring the rate of change of P_z and M_z to be equal to resultant external load and torque per unit length, P_{z1} and M_{z1} , of the prescribed axial and circumferential shears, i.e.,

$$\frac{\partial P_z}{\partial z} + P_{z1} = 0 \quad \text{and} \quad \frac{\partial M_z}{\partial z} + M_{z1} = 0. \tag{50}$$

Differentiating Eq. (49) and enforcing Eq. (50) yields

$$\begin{bmatrix} \kappa_{133} & \kappa_{136} \\ \kappa_{136} & \kappa_{166} \end{bmatrix} \left\{ \begin{array}{l} a_{13} \\ a_{16} \end{array} \right\} + \left\{ \begin{array}{l} P_{IIP1} \\ M_{IIP1} \end{array} \right\} + \sum_{\alpha=1}^2 c_{I\alpha} \left\{ \begin{array}{l} P_{IIE\alpha} \\ M_{IIE\alpha} \end{array} \right\} + \left\{ \begin{array}{l} P_{z1} \\ M_{z1} \end{array} \right\} = 0. \tag{51}$$

Setting $z = 0$ in Eq. (49) gives an expression involving $P_z(0)$ and $M_z(0)$, i.e., the applied axial force and torque at the tip end, as

$$\begin{aligned}
& \begin{bmatrix} \kappa_{II33} & \kappa_{II36} \\ \kappa_{II36} & \kappa_{II66} \end{bmatrix} \left\{ \begin{array}{l} a_{13} \\ a_{16} \end{array} \right\} + \begin{bmatrix} \kappa_{133} & \kappa_{136} \\ \kappa_{136} & \kappa_{166} \end{bmatrix} \left\{ \begin{array}{l} a_{II3} \\ a_{II6} \end{array} \right\} + \left\{ \begin{array}{l} P_{IIP2} \\ M_{IIP2} \end{array} \right\} + \sum_{\alpha} c_{I\alpha} \left\{ \begin{array}{l} P_{IE\alpha} \\ M_{IE\alpha} \end{array} \right\} + \sum_{\alpha} c_{II\alpha} \left\{ \begin{array}{l} P_{IE\alpha} \\ M_{IE\alpha} \end{array} \right\} \\
& = \left\{ \begin{array}{l} P_z(0) \\ M_z(0) \end{array} \right\}.
\end{aligned} \tag{52}$$

Such tip-end loads were considered in Problem I, and can be set equal to zero in this calculation. Surface electric conditions must be appended to these equations before a solution is possible. These conditions are treated in the sequel.

6.2. Both surfaces open

No electrical terms are needed in \mathbf{V}_1 of Eq. (43), so that Eq. (51) takes the form

$$\begin{bmatrix} \kappa_{133} & \kappa_{136} \\ \kappa_{136} & \kappa_{166} \end{bmatrix} \left\{ \begin{array}{l} a_{13} \\ a_{16} \end{array} \right\} = - \left\{ \begin{array}{l} P_{IIP1} + P_{z1} \\ M_{IIP1} + M_{z1} \end{array} \right\}. \tag{53}$$

After determining a_{13} and a_{16} , Eq. (52) is used for finding a_{II3} and a_{II6} . To wit

$$\begin{bmatrix} \kappa_{I33} & \kappa_{I36} \\ \kappa_{I36} & \kappa_{I66} \end{bmatrix} \begin{Bmatrix} a_{II3} \\ a_{II6} \end{Bmatrix} = - \begin{bmatrix} \kappa_{II33} & \kappa_{II36} \\ \kappa_{II36} & \kappa_{II66} \end{bmatrix} \begin{Bmatrix} a_{13} \\ a_{16} \end{Bmatrix} - \begin{Bmatrix} P_{IIP2} \\ M_{IIP2} \end{Bmatrix}. \quad (54)$$

6.3. Linearly varying voltages on both surfaces

Let the inside and outside lateral surfaces have distinct linear voltage gradients along z at rates of $\overline{\Delta\phi}_i$ and $\overline{\Delta\phi}_o$. Also, assume that the electric potentials on the inside and outside surfaces at $z = 0$ are zero. No generality is lost, since non-zero uniform potentials, $\bar{\phi}_i$ and $\bar{\phi}_o$, can be taken into account by the superposition of Problem I. For prescribed potential gradients $\Delta\phi_i$ and $\Delta\phi_o$, the two potential gradient expressions, obtained through the differentiation of Eq. (43), are

$$\begin{aligned} \psi_{13\phi}(r_i)a_{13} + \psi_{16\phi}(r_i)a_{16} + U_{IE1\phi}(r_i)c_{11} + U_{IE2\phi}(r_i)c_{12} + U_{IIP1\phi}(r_i) &= \overline{\Delta\phi}_i, \\ \psi_{13\phi}(r_o)a_{13} + \psi_{16\phi}(r_o)a_{16} + U_{IE1\phi}(r_o)c_{11} + U_{IE2\phi}(r_o)c_{12} + U_{IIP1\phi}(r_o) &= \overline{\Delta\phi}_o. \end{aligned} \quad (55)$$

These expressions along with Eq. (51) constitute the four equations for a_{13} , a_{16} , c_{11} , and c_{12} , given as

$$\begin{bmatrix} \kappa_{I33} & \kappa_{I36} & P_{IE1} & P_{IE2} \\ \kappa_{I36} & \kappa_{I66} & M_{IE1} & M_{IE2} \\ \psi_{13\phi}(r_i) & \psi_{16\phi}(r_i) & U_{IE1\phi}(r_i) & U_{IE2\phi}(r_i) \\ \psi_{13\phi}(r_o) & \psi_{16\phi}(r_o) & U_{IE1\phi}(r_o) & U_{IE2\phi}(r_o) \end{bmatrix} \begin{Bmatrix} a_{13} \\ a_{16} \\ c_{11} \\ c_{12} \end{Bmatrix} = \begin{Bmatrix} -(P_{IIP1} + P_{z1}) \\ -(M_{IIP1} + M_{z1}) \\ \overline{\Delta\phi}_i - U_{IIP1\phi}(r_i) \\ \overline{\Delta\phi}_o - U_{IIP1\phi}(r_o) \end{Bmatrix}. \quad (56)$$

Next, Eq. (52) with $\overline{\phi}_i = 0$ and $\overline{\phi}_o = 0$ in Eq. (43) provides the means for determining a_{II3} , a_{II6} , c_{II1} , and c_{II2} . Thus

$$\begin{aligned} \begin{bmatrix} \kappa_{I33} & \kappa_{I36} & P_{IE1} & P_{IE2} \\ \kappa_{I36} & \kappa_{I66} & M_{IE1} & M_{IE2} \\ \psi_{13\phi}(r_i) & \psi_{16\phi}(r_i) & U_{IE1\phi}(r_i) & U_{IE2\phi}(r_i) \\ \psi_{13\phi}(r_o) & \psi_{16\phi}(r_o) & U_{IE1\phi}(r_o) & U_{IE2\phi}(r_o) \end{bmatrix} \begin{Bmatrix} a_{II3} \\ a_{II6} \\ c_{II1} \\ c_{II2} \end{Bmatrix} \\ = - \begin{Bmatrix} P_{IIP2} \\ M_{IIP2} \\ U_{IIP2\phi}(r_i) \\ U_{IIP2\phi}(r_o) \end{Bmatrix} - \begin{bmatrix} \kappa_{II33} & \kappa_{II36} & P_{IIE1} & P_{IIE2} \\ \kappa_{II36} & \kappa_{II66} & M_{IIE1} & M_{IIE2} \\ \psi_{II3\phi}(r_i) & \psi_{II6\phi}(r_i) & U_{IIE1\phi}(r_i) & U_{IIE2\phi}(r_i) \\ \psi_{II3\phi}(r_o) & \psi_{II6\phi}(r_o) & U_{IIE1\phi}(r_o) & U_{IIE2\phi}(r_o) \end{bmatrix} \begin{Bmatrix} a_{13} \\ a_{16} \\ c_{11} \\ c_{12} \end{Bmatrix}. \end{aligned} \quad (57)$$

6.4. Linearly varying electric displacement on both surfaces

Let $\overline{\Delta D}_i(r_i)$ and $\overline{\Delta D}_o(r_o)$ be prescribed gradients of electric charges on the inside and outside surfaces. Enforcing this condition with Eq. (48) leads to

$$\begin{aligned} D_{I3r}(r_i)a_{13} + D_{I6r}(r_i)a_{16} + D_{IE1r}(r_i)c_{11} + D_{IE2r}(r_i)c_{12} + D_{IIP1r}(r_i) &= \overline{\Delta D}_i, \\ D_{I3r}(r_o)a_{13} + D_{I6r}(r_o)a_{16} + D_{IE1r}(r_o)c_{11} + D_{IE2r}(r_o)c_{12} + D_{IIP1r}(r_o) &= \overline{\Delta D}_o. \end{aligned} \quad (58)$$

These relations, together with Eq. (51), give the four equations for a_{13} , a_{16} , c_{11} , and c_{12} . Thus

$$\begin{bmatrix} \kappa_{I33} & \kappa_{I36} & P_{IE1} & P_{IE2} \\ \kappa_{I36} & \kappa_{I66} & M_{IE1} & M_{IE2} \\ D_{I3r}(r_i) & D_{I6r}(r_i) & D_{IE1r}(r_i) & D_{IE2r}(r_i) \\ D_{I3r}(r_o) & D_{I6r}(r_o) & D_{IE1r}(r_o) & D_{IE2r}(r_o) \end{bmatrix} \begin{Bmatrix} a_{13} \\ a_{16} \\ c_{11} \\ c_{12} \end{Bmatrix} = \begin{Bmatrix} -(P_{IIP1} + P_{z1}) \\ -(M_{IIP1} + M_{z1}) \\ \overline{\Delta D}_i - D_{IIP1r}(r_i) \\ \overline{\Delta D}_o - D_{IIP1r}(r_o) \end{Bmatrix}. \quad (59)$$

The electric displacement D_r on the outside and inside surfaces may be assumed to be zero as non-vanishing values were already considered in Problem I. Evaluating D_{r_i} and D_{r_o} at $z = 0$ by Eq. (48) and setting them equal to zero yields

$$\begin{aligned} D_{II3r}(r_i)a_{i3} + D_{II6r}(r_i)a_{i6} + D_{IIE1r}(r_i)c_{i1} + D_{IIE2r}(r_i)c_{i2} + D_{IIP2r}(r_i) + D_{I3r}(r_i)a_{II3} + D_{I6r}(r_i)a_{II6} \\ + D_{IE1r}(r_i)c_{II1} + D_{IE2r}(r_i)c_{II2} = 0, \\ D_{II3r}(r_o)a_{i3} + D_{II6r}(r_o)a_{i6} + D_{IIE1r}(r_o)c_{i1} + D_{IIE2r}(r_o)c_{i2} \\ + D_{IIP2r}(r_o) + D_{I3r}(r_o)a_{II3} + D_{I6r}(r_o)a_{II6} + D_{IE1r}(r_o)c_{II1} + D_{IE2r}(r_o)c_{II2} = 0. \end{aligned} \quad (60)$$

Combining these equations with Eq. (52), the equations for a_{II3} , a_{II6} , c_{II1} and c_{II2} are obtained as

$$\begin{aligned} & \begin{bmatrix} \kappa_{I33} & \kappa_{I36} & P_{IE1} & P_{IE2} \\ \kappa_{I36} & \kappa_{I66} & M_{IE1} & M_{IE2} \\ D_{I3r}(r_i) & D_{I6r}(r_i) & D_{IE1r}(r_i) & D_{IE2r}(r_i) \\ D_{I3r}(r_o) & D_{I6r}(r_o) & D_{IE1r}(r_o) & D_{IE2r}(r_o) \end{bmatrix} \begin{Bmatrix} a_{II3} \\ a_{II6} \\ c_{II1} \\ c_{II2} \end{Bmatrix} \\ &= - \begin{Bmatrix} P_{IIP2} \\ M_{IIP2} \\ D_{IIP2r}(r_i) \\ D_{IIP2r}(r_o) \end{Bmatrix} - \begin{bmatrix} \kappa_{II33} & \kappa_{II36} & P_{IIE1} & P_{IIE2} \\ \kappa_{II36} & \kappa_{II66} & M_{IIE1} & M_{IIE2} \\ D_{II3r}(r_i) & D_{II6r}(r_i) & D_{IIE1r}(r_i) & D_{IIE2r}(r_i) \\ D_{II3r}(r_o) & D_{II6r}(r_o) & D_{IIE1r}(r_o) & D_{IIE2r}(r_o) \end{bmatrix} \begin{Bmatrix} a_{i3} \\ a_{i6} \\ c_{i1} \\ c_{i2} \end{Bmatrix}. \end{aligned} \quad (61)$$

6.5. Validation example for problem II

We shall analyze a homogeneous circular cylinder with the same geometry used for the validation problem earlier. However, we will use a crystal orientation angle $\Theta = 90^\circ$ in this example.² Thus, the elastic stiffness moduli (in Pascals) are given as, $c_{11} = c_{22} = 127 \times 10^9$, $c_{33} = 117 \times 10^9$, $c_{44} = c_{55} = 23.0 \times 10^9$, $c_{66} = 23.5 \times 10^9$, $c_{12} = 80.2 \times 10^9$, $c_{13} = c_{23} = 84.7 \times 10^9$; the piezoelectric moduli (in Coulomb/m²) are given as $e_{11} = e_{22} = e_{33} = 1.5 \times 10^{-8}$; and the dielectric permittivity constants (in Farad/m) are given as $\epsilon_{13} = \epsilon_{23} = -6.1$, $\epsilon_{33} = 15.7$.

The cylinder is subjected to uniform outside circumferential shear tractions, $\bar{\sigma}_{\theta o} = 1.0$ Pa; uniform outside axial shear tractions, $\bar{\sigma}_{zo} = 1.0$ Pa; linearly varying outside surface voltage and pressure distributions with $\bar{\Delta\phi}_o = 5$ V/L, and $\bar{\Delta\sigma}_{ro} = 5$ Pa/L. Thus, for example, the outside pressure is $\bar{\sigma}_{ro} = 0$ at $z = 0$, and $\bar{\sigma}_{ro} = 100$ at $z = L$. To the best of the authors' knowledge, analytical solutions of these problems do not exist. So the semi-analytic results are compared with those obtained with the finite element method (ANSYS, 1998). The variation of the stresses, displacements and potential through the thickness of the cylinder, normalized with their respective maximum values, as computed via the two methods are displayed in Fig. 5. The agreement between these two results are, again, quite good.

Note that, the comparisons in this problem are made at the mid-length of the cylinder, away from the two ends where the end-effects are observed. The treatment of the end-effects is possible with the semi-analytic method, and is deferred to a subsequent publication.

Also note that, the free-surface integral of the normal electric displacements defined in Eq. (17) yield the values of $\{3.9 \times 10^{-12}, 1.1 \times 10^{-9}, 1.9 \times 10^{-13}, 0.0\}$ Coulombs for the linear pressure, linear potential, uniform axial and uniform torsional shear problems, respectively. The corresponding largest individual integrated free-surface fluxes—either of left-face, right-face, interior or exterior surfaces—are $\{6.1 \times 10^{-8}, 2.3 \times 10^{-5}$,

² Note that $\Theta = 0^\circ$ for the first verification problem.

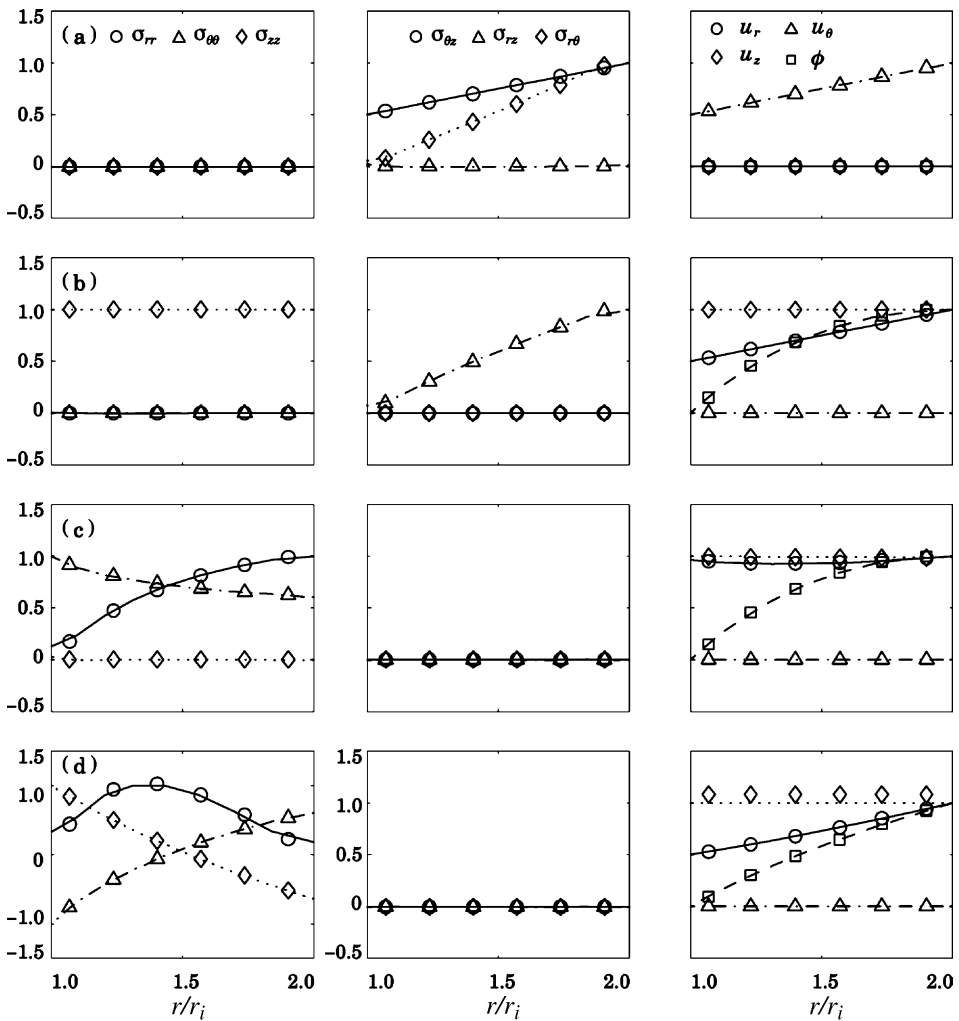


Fig. 5. Validation for Problem II: the results are for uniform circumferential (Row a) and axial (Row b) shear tractions, as well as linear pressure (Row c) and voltage (Row d) distributions prescribed on the exterior surface of the cylinder. The symbols and the (dashed, dotted, etc.) lines denote the semi-analytic and ANSYS results at the mid-length of the cylinder, respectively.

$9.2 \times 10^{-8}, 0.0\}$ Coulombs, respectively. Again, the total values (which are ideally equal to zero) are roughly four orders of magnitude smaller than the individual values, thereby validating the consistency of the semi-analytic method.

7. Problem III—quadratically varying state

The parabolically varying state is governed by Eq. (15.2) whose explicit form is

$$\mathbf{K}_1 \mathbf{V}_2 + \mathbf{K}_3 \mathbf{V}_{2,z} - \mathbf{K}_6 \mathbf{V}_{2,zz} = \mathbf{F}_{2c0} + z(\mathbf{F}_{1b} + \mathbf{F}_{2c0}) + z^2(\mathbf{F}_{2a} + \mathbf{F}_{2c0}). \quad (62)$$

7.1. Analysis

The analysis procedure follows the previous strategy. There is a cascading of the generalized coordinates, warpage functions, particular solutions and electric vectors. As the formulation is parallel to the two previous problems, we will not dwell on the details unless an issue is clearly new to the discussion of the analysis.

The most general form of the displacement field for Eq. (62) is obtained by integrating Eq. (43) once with respect to z . Thus,

$$\begin{aligned}
 \mathbf{V}_2 = & a_{13} \left(\frac{z^3}{6} \mathbf{R}_3 + \frac{z^2}{2} \mathbf{\Psi}_{13} + z \mathbf{\Psi}_{II3} + \mathbf{\Psi}_{III3} \right) + a_{16} \left(\frac{z^3}{6} \mathbf{R}_6 + \frac{z^2}{2} \mathbf{\Psi}_{16} + a \mathbf{\Psi}_{II6} + \mathbf{\Psi}_{III6} \right) \\
 & + a_{II3} \left(\frac{z^2}{2} \mathbf{R}_3 + z \mathbf{\Psi}_{13} + \mathbf{\Psi}_{II3} \right) + a_{II6} \left(\frac{z^2}{2} \mathbf{R}_6 + z \mathbf{\Psi}_{16} + \mathbf{\Psi}_{II6} \right) + a_{III3} (z \mathbf{R}_3 + \mathbf{\Psi}_{13}) + a_{III6} (z \mathbf{R}_6 + \mathbf{\Psi}_{16}) \\
 & + \frac{z^2}{2} \mathbf{U}_{IIIP1} + z \mathbf{U}_{IIIP2} + \mathbf{U}_{IIIP3} + \sum_{\alpha} \left[c_{I\alpha} \left(\frac{z^2}{2} \mathbf{U}_{IE\alpha} + z \mathbf{U}_{IIE\alpha} + \mathbf{U}_{III\alpha} \right) + c_{II\alpha} (z \mathbf{U}_{IE\alpha} + \mathbf{U}_{IIE\alpha}) + c_{III\alpha} \mathbf{U}_{IE\alpha} \right] \\
 & + \mathbf{\Phi}_{RB} \mathbf{a}_{RB},
 \end{aligned} \tag{63}$$

where $(a_{1i}, a_{IIi}, a_{IIIi}, c_{Ii}, c_{IIi}, c_{IIIi}, i = 3, 6)$ are generalized deformation coordinates. Substituting Eq. (62) into (15.2) leads to all of the defining equations, among which those for $\mathbf{\Psi}_{III3}$, $\mathbf{\Psi}_{III6}$, \mathbf{U}_{IIIPi} , $i = 1, 2, 3$ and $\mathbf{U}_{III\alpha}$, $\alpha = 1, 2$ are new. These are determined by solving the following equations

$$\mathbf{K}_1 \mathbf{\Psi}_{III3} + \mathbf{K}_3 \mathbf{\Psi}_{13} - \mathbf{K}_6 \mathbf{\Psi}_{13} = 0, \quad \mathbf{K}_1 \mathbf{\Psi}_{III6} + \mathbf{K}_3 \mathbf{\Psi}_{16} - \mathbf{K}_6 \mathbf{\Psi}_{16} = 0, \tag{64}$$

$$\mathbf{K}_1 \mathbf{U}_{IIIP1} - 2 \mathbf{F}_{2a1} = 0, \quad \mathbf{K}_1 \mathbf{U}_{IIIP2} + \mathbf{K}_3 \mathbf{U}_{IIIP1} - \mathbf{F}_{1b1} = 0, \quad \mathbf{K}_1 \mathbf{U}_{IIIP3} + \mathbf{K}_3 \mathbf{U}_{IIIP2} - \mathbf{K}_6 \mathbf{U}_{IIIP1} = 0, \tag{65}$$

$$\mathbf{K}_1 \mathbf{U}_{III\alpha} + \mathbf{K}_3 \mathbf{U}_{IIE\alpha} - \mathbf{K}_6 \mathbf{U}_{IE\alpha} = 0 \quad (\alpha = 1, 2). \tag{66}$$

The quadratic stress and electric displacement field for this case is

$$\begin{aligned}
 \mathbf{Q} = & \frac{z^2}{2} C^* [a_{13} (\mathbf{b}_r \mathbf{\Psi}_{13} + \mathbf{b}_z \mathbf{r}_3) + a_{16} (\mathbf{b}_r \mathbf{\Psi}_{16} + \mathbf{b}_z \mathbf{r}_6) + \mathbf{b}_r \mathbf{U}_{IIIP1}] + z C^* [a_{13} (\mathbf{b}_r \mathbf{\Psi}_{II3} + \mathbf{b}_z \mathbf{\Psi}_{13}) \\
 & + a_{16} (\mathbf{b}_r \mathbf{\Psi}_{II6} + \mathbf{b}_z \mathbf{\Psi}_{16}) + a_{II3} (\mathbf{b}_r \mathbf{\Psi}_{13} + \mathbf{b}_z \mathbf{r}_3) + a_{II6} (\mathbf{b}_r \mathbf{\Psi}_{16} + \mathbf{b}_z \mathbf{r}_6) + \mathbf{b}_r \mathbf{U}_{IIIP2} + \mathbf{b}_z \mathbf{U}_{IIIP1}] \\
 & + C^* [a_{13} (\mathbf{b}_r \mathbf{\Psi}_{III3} + \mathbf{b}_z \mathbf{\Psi}_{II3}) + a_{16} (\mathbf{b}_r \mathbf{\Psi}_{III6} + \mathbf{b}_z \mathbf{\Psi}_{II6}) + a_{II3} (\mathbf{b}_r \mathbf{\Psi}_{II3} + \mathbf{b}_z \mathbf{\Psi}_{13}) + a_{II6} (\mathbf{b}_r \mathbf{\Psi}_{II6} + \mathbf{b}_z \mathbf{\Psi}_{16}) \\
 & + a_{III3} (\mathbf{b}_r \mathbf{\Psi}_{13} + \mathbf{b}_z \mathbf{r}_3) + a_{III6} (\mathbf{b}_r \mathbf{\Psi}_{16} + \mathbf{b}_z \mathbf{r}_6) + \mathbf{b}_r \mathbf{U}_{IIIP3} + \mathbf{b}_z \mathbf{U}_{IIIP2}] + \frac{z^2}{2} C^* \sum_{\alpha=1}^2 c_{I\alpha} \mathbf{b}_r \mathbf{U}_{IE\alpha} \\
 & + z C^* \sum_{\alpha=1}^2 [c_{I\alpha} (\mathbf{b}_r \mathbf{U}_{IIE\alpha} + \mathbf{b}_z \mathbf{U}_{IE\alpha}) + c_{II\alpha} \mathbf{b}_r \mathbf{U}_{IE\alpha}] \\
 & + C^* \sum_{\alpha=1}^2 [c_{I\alpha} (\mathbf{b}_r \mathbf{U}_{III\alpha} + \mathbf{b}_z \mathbf{U}_{IIE\alpha}) + c_{II\alpha} (\mathbf{b}_r \mathbf{U}_{IIE\alpha} + \mathbf{b}_z \mathbf{U}_{IE\alpha}) + c_{III\alpha} \mathbf{b}_r \mathbf{U}_{IE\alpha}].
 \end{aligned} \tag{67}$$

Integrating σ_{zz} and $\sigma_{\theta z}$ over a generic cross-section according to Eq. (16) yields

$$\begin{aligned} \left\{ \begin{array}{l} P_z(z) \\ M_z(z) \end{array} \right\} = & \frac{z^2}{2} \left(\begin{bmatrix} \kappa_{I33} & \kappa_{I36} \\ \kappa_{I36} & \kappa_{I66} \end{bmatrix} \left\{ \begin{array}{l} a_{I3} \\ a_{I6} \end{array} \right\} + \left\{ \begin{array}{l} P_{IIP1} \\ M_{IIP1} \end{array} \right\} \right) + z \left(\begin{bmatrix} \kappa_{II33} & \kappa_{II36} \\ \kappa_{II36} & \kappa_{II66} \end{bmatrix} \left\{ \begin{array}{l} a_{I3} \\ a_{I6} \end{array} \right\} + \begin{bmatrix} \kappa_{I33} & \kappa_{I36} \\ \kappa_{I36} & \kappa_{I66} \end{bmatrix} \left\{ \begin{array}{l} a_{II3} \\ a_{II6} \end{array} \right\} \right. \right. \\ & \left. \left. + \left\{ \begin{array}{l} P_{IIP2} \\ M_{IIP2} \end{array} \right\} \right) + \begin{bmatrix} \kappa_{I33} & \kappa_{I36} \\ \kappa_{I36} & \kappa_{I66} \end{bmatrix} \left\{ \begin{array}{l} a_{III3} \\ a_{III6} \end{array} \right\} + \begin{bmatrix} \kappa_{II33} & \kappa_{II36} \\ \kappa_{II36} & \kappa_{II66} \end{bmatrix} \left\{ \begin{array}{l} a_{II3} \\ a_{II6} \end{array} \right\} + \begin{bmatrix} \kappa_{III33} & \kappa_{III36} \\ \kappa_{III36} & \kappa_{III66} \end{bmatrix} \left\{ \begin{array}{l} a_{I3} \\ a_{I6} \end{array} \right\} \right. \right. \\ & \left. \left. + \left\{ \begin{array}{l} P_{IIP3} \\ M_{IIP3} \end{array} \right\} + \frac{z^2}{2} \sum_{\alpha} c_{I\alpha} \left\{ \begin{array}{l} P_{IE\alpha} \\ M_{IE\alpha} \end{array} \right\} + z \sum_{\alpha} c_{I\alpha} \left\{ \begin{array}{l} P_{IIE\alpha} \\ M_{IIE\alpha} \end{array} \right\} + z \sum_{\alpha} c_{II\alpha} \left\{ \begin{array}{l} P_{IE\alpha} \\ M_{IE\alpha} \end{array} \right\} \right. \right. \\ & \left. \left. + \sum_{\alpha} c_{I\alpha} \left\{ \begin{array}{l} P_{IIIIE\alpha} \\ M_{IIIIE\alpha} \end{array} \right\} + \sum_{\alpha} c_{II\alpha} \left\{ \begin{array}{l} P_{IIE\alpha} \\ M_{IIE\alpha} \end{array} \right\} + \sum_{\alpha} c_{III\alpha} \left\{ \begin{array}{l} P_{IE\alpha} \\ M_{IE\alpha} \end{array} \right\} \right), \end{aligned} \quad (68)$$

where κ_{IIIij} 's and the mechanical and electric load resultants have the same formulas as those given by Eqs. (33)–(35) except with the stresses in these formulas replaced by their corresponding components with the appropriate subscripts, for example,

$$\begin{aligned} \kappa_{III33} &= 2\pi \sum_{m=1}^M \int \sigma_{zzIII3} r dr, \\ P_{IIP\gamma} &= 2\pi \sum_{m=1}^M \int \sigma_{zz(IIP\gamma)} r dr \quad (\gamma = 1, 2, 3), \\ P_{IIE\alpha} &= 2\pi \sum_{m=1}^M \int \sigma_{zz(EIIE\alpha)} r dr \quad (\alpha = 1, 2). \end{aligned} \quad (69)$$

Eq. (68) gives axial force P_z and torque M_z at any z in terms of the generalized coordinates. These coordinates for the quadratically varying field are determined in three stages. The second derivative of Eq. (68) must be equal to the circumferential integral of the linearly varying applied surface tractions, P_{z2} and M_{z2} , that possess axial resultants. Thus

$$\frac{\partial^2 P_z}{\partial z^2} + P_{z2} = 0; \quad \frac{\partial^2 M_z}{\partial z^2} + M_{z2} = 0. \quad (70)$$

Differentiating Eq. (68) twice with respect to the axial coordinate z and enforcing this global equilibrium condition yields

$$\begin{bmatrix} \kappa_{I33} & \kappa_{I36} \\ \kappa_{I36} & \kappa_{I66} \end{bmatrix} \left\{ \begin{array}{l} a_{I3} \\ a_{I6} \end{array} \right\} + \sum_{\alpha=1}^2 c_{I\alpha} \left\{ \begin{array}{l} P_{IE\alpha} \\ M_{IE\alpha} \end{array} \right\} + \left\{ \begin{array}{l} P_{IIP1} \\ M_{IIP1} \end{array} \right\} + \left\{ \begin{array}{l} P_{z2} \\ M_{z2} \end{array} \right\} = 0. \quad (71)$$

The first derivative of Eq. (68) evaluated at $z = 0$ gives the expressions to be equated to the resultants of the uniformly applied surface tractions with axial resultants. Since such applied tractions were treated in Problem II, they are omitted here. Therefore

$$\frac{\partial P_z}{\partial z} = 0, \quad \frac{\partial M_z}{\partial z} = 0. \quad (72)$$

Carrying out this evaluation by differentiating Eq. (68) gives

$$\begin{aligned} & \begin{bmatrix} \kappa_{II33} & \kappa_{II36} \\ \kappa_{II36} & \kappa_{II66} \end{bmatrix} \left\{ \begin{array}{l} a_{I3} \\ a_{I6} \end{array} \right\} + \begin{bmatrix} \kappa_{I33} & \kappa_{I36} \\ \kappa_{I36} & \kappa_{I66} \end{bmatrix} \left\{ \begin{array}{l} a_{II3} \\ a_{II6} \end{array} \right\} + \sum_{\alpha} c_{I\alpha} \left\{ \begin{array}{l} P_{IIE\alpha} \\ M_{IIE\alpha} \end{array} \right\} \\ & + \sum_{\alpha} c_{II\alpha} \left\{ \begin{array}{l} P_{IE\alpha} \\ M_{IE\alpha} \end{array} \right\} + \left\{ \begin{array}{l} P_{IIP2} \\ M_{IIP2} \end{array} \right\} = 0. \end{aligned} \quad (73)$$

Finally, evaluating Eq. (68) at $z = 0$ gives the value of P_z and M_z at the tip end. These loads were considered in Problem I and can be set equal to zero here. Thus, this condition yields

$$\begin{bmatrix} \kappa_{III33} & \kappa_{III36} \\ \kappa_{III36} & \kappa_{III66} \end{bmatrix} \begin{Bmatrix} a_{I3} \\ a_{I6} \end{Bmatrix} + \begin{bmatrix} \kappa_{II33} & \kappa_{II36} \\ \kappa_{II36} & \kappa_{II66} \end{bmatrix} \begin{Bmatrix} a_{II3} \\ a_{II6} \end{Bmatrix} + \begin{bmatrix} \kappa_{I33} & \kappa_{I36} \\ \kappa_{I36} & \kappa_{I66} \end{bmatrix} \begin{Bmatrix} a_{III3} \\ a_{III6} \end{Bmatrix} + \sum_{\alpha} c_{I\alpha} \begin{Bmatrix} P_{III\alpha} \\ M_{III\alpha} \end{Bmatrix} + \sum_{\alpha} c_{II\alpha} \begin{Bmatrix} P_{II\alpha} \\ M_{II\alpha} \end{Bmatrix} + \sum_{\alpha} c_{III\alpha} \begin{Bmatrix} P_{I\alpha} \\ M_{I\alpha} \end{Bmatrix} + \begin{Bmatrix} P_{IIP3} \\ M_{IIP3} \end{Bmatrix} = 0. \quad (74)$$

Eqs. (71), (73) and (74) must be supplemented by electric surface conditions. These are considered in the sequel.

7.2. Both surfaces open

For this case, no electric fields are involved; hence $c_{I\alpha} = c_{II\alpha} = c_{III\alpha} = 0$. Equations (71), (73) and (74) become

$$\begin{bmatrix} \kappa_{I33} & \kappa_{I36} \\ \kappa_{I36} & \kappa_{I66} \end{bmatrix} \begin{Bmatrix} a_{I3} \\ a_{I6} \end{Bmatrix} + \begin{Bmatrix} P_{IIP1} \\ M_{IIP1} \end{Bmatrix} + \begin{Bmatrix} P_{z2} \\ M_{z2} \end{Bmatrix} = 0, \quad (75)$$

$$\begin{bmatrix} \kappa_{II33} & \kappa_{II36} \\ \kappa_{II36} & \kappa_{II66} \end{bmatrix} \begin{Bmatrix} a_{I3} \\ a_{I6} \end{Bmatrix} + \begin{bmatrix} \kappa_{II33} & \kappa_{II36} \\ \kappa_{II36} & \kappa_{II66} \end{bmatrix} \begin{Bmatrix} a_{II3} \\ a_{II6} \end{Bmatrix} + \begin{Bmatrix} P_{IIP2} \\ M_{IIP2} \end{Bmatrix} = 0, \quad (76)$$

$$\begin{bmatrix} \kappa_{III33} & \kappa_{III36} \\ \kappa_{III36} & \kappa_{III66} \end{bmatrix} \begin{Bmatrix} a_{I3} \\ a_{I6} \end{Bmatrix} + \begin{bmatrix} \kappa_{III33} & \kappa_{III36} \\ \kappa_{III36} & \kappa_{III66} \end{bmatrix} \begin{Bmatrix} a_{II3} \\ a_{II6} \end{Bmatrix} + \begin{bmatrix} \kappa_{I33} & \kappa_{I36} \\ \kappa_{I36} & \kappa_{I66} \end{bmatrix} \begin{Bmatrix} a_{III3} \\ a_{III6} \end{Bmatrix} + \begin{Bmatrix} P_{IIP3} \\ M_{IIP3} \end{Bmatrix} = 0. \quad (77)$$

The sequential solutions of these equations yield a_{I3} , a_{I6} , a_{II3} , a_{II6} , a_{III3} , and a_{III6} .

7.3. Quadratically varying voltages on both surfaces

Let the inside and outside lateral surfaces have distinct quadratic voltage distributions along z , given by

$$\phi_i(z) = \frac{z^2}{2} \overline{\Delta^2 \phi_i} + z \overline{\Delta \phi_i} + \bar{\phi}_i, \quad \phi_o(z) = \frac{z^2}{2} \overline{\Delta^2 \phi_o} + z \overline{\Delta \phi_o} + \bar{\phi}_o. \quad (78)$$

Similar to the discussion in Problem II, application of the boundary conditions via two differentiations of Eq. (63) and the rearrangement of these results together with Eqs. (71), (73) and (74) give

$$\begin{bmatrix} \kappa_{I33} & \kappa_{I36} & P_{IE1} & P_{IE2} \\ \kappa_{I36} & \kappa_{I66} & M_{IE1} & M_{IE2} \\ \psi_{13\phi}(r_i) & \psi_{16\phi}(r_i) & U_{IE1\phi}(r_i) & U_{IE2\phi}(r_i) \\ \psi_{13\phi}(r_o) & \psi_{16\phi}(r_o) & U_{IE1\phi}(r_o) & U_{IE2\phi}(r_o) \end{bmatrix} \begin{Bmatrix} a_{I3} \\ a_{I6} \\ c_{II} \\ c_{II2} \end{Bmatrix} = \begin{Bmatrix} -(P_{IIP1} + P_{z2}) \\ -(M_{IIP1} + M_{z2}) \\ 2\overline{\Delta^2 \phi_i} - U_{IIP1\phi}(r_i) \\ 2\overline{\Delta^2 \phi_o} - U_{IIP1\phi}(r_o) \end{Bmatrix}, \quad (79)$$

$$\begin{bmatrix} \kappa_{I33} & \kappa_{I36} & P_{IE1} & P_{IE2} \\ \kappa_{I36} & \kappa_{I66} & M_{IE1} & M_{IE2} \\ \psi_{13\phi}(r_i) & \psi_{16\phi}(r_i) & U_{IE1\phi}(r_i) & U_{IE2\phi}(r_i) \\ \psi_{13\phi}(r_o) & \psi_{16\phi}(r_o) & U_{IE1\phi}(r_o) & U_{IE2\phi}(r_o) \end{bmatrix} \begin{Bmatrix} a_{II3} \\ a_{II6} \\ c_{III} \\ c_{II2} \end{Bmatrix} = - \begin{Bmatrix} P_{IIP2} \\ M_{IIP2} \\ U_{IIP2\phi}(r_i) \\ U_{IIP2\phi}(r_o) \end{Bmatrix} - \begin{bmatrix} \kappa_{II33} & \kappa_{II36} & P_{IE1} & P_{IE2} \\ \kappa_{II36} & \kappa_{II66} & M_{IE1} & M_{IE2} \\ \psi_{II3\phi}(r_i) & \psi_{II6\phi}(r_i) & U_{IE1\phi}(r_i) & U_{IE2\phi}(r_i) \\ \psi_{II3\phi}(r_o) & \psi_{II6\phi}(r_o) & U_{IE1\phi}(r_o) & U_{IE2\phi}(r_o) \end{bmatrix} \begin{Bmatrix} a_{I6} \\ c_{II1} \\ c_{II2} \end{Bmatrix}, \quad (80)$$

$$\begin{aligned}
& \begin{bmatrix} \kappa_{133} & \kappa_{136} & P_{1E1} & P_{1E2} \\ \kappa_{136} & \kappa_{166} & M_{1E1} & M_{1E2} \\ \psi_{13\phi}(r_i) & \psi_{16\phi}(r_i) & U_{1E1\phi}(r_i) & U_{1E2\phi}(r_i) \\ \psi_{13\phi}(r_o) & \psi_{16\phi}(r_o) & U_{1E1\phi}(r_o) & U_{1E2\phi}(r_o) \end{bmatrix} \begin{Bmatrix} a_{III3} \\ a_{III6} \\ c_{III1} \\ c_{III2} \end{Bmatrix} \\
&= - \begin{Bmatrix} P_{IIP3} \\ M_{IIP3} \\ U_{IIP3\phi}(r_i) \\ U_{IIP3\phi}(r_o) \end{Bmatrix} - \begin{bmatrix} \kappa_{II33} & \kappa_{II36} & P_{IIE1} & P_{IIE2} \\ \kappa_{II36} & \kappa_{II66} & M_{IIE1} & M_{IIE2} \\ \psi_{II3\phi}(r_i) & \psi_{II6\phi}(r_i) & U_{IIE1\phi}(r_i) & U_{IIE2\phi}(r_i) \\ \psi_{II3\phi}(r_o) & \psi_{II6\phi}(r_o) & U_{IIE1\phi}(r_o) & U_{IIE2\phi}(r_o) \end{bmatrix} \begin{Bmatrix} a_{II3} \\ a_{II6} \\ c_{II1} \\ c_{II2} \end{Bmatrix} \\
&\quad - \begin{bmatrix} \kappa_{III33} & \kappa_{III36} & P_{IIIIE1} & P_{IIIIE2} \\ \kappa_{III36} & \kappa_{III66} & M_{IIIIE1} & M_{IIIIE2} \\ \psi_{III3\phi}(r_i) & \psi_{III6\phi}(r_i) & U_{IIIIE1\phi}(r_i) & U_{IIIIE2\phi}(r_i) \\ \psi_{III3\phi}(r_o) & \psi_{III6\phi}(r_o) & U_{IIIIE1\phi}(r_o) & U_{IIIIE2\phi}(r_o) \end{bmatrix} \begin{Bmatrix} a_{I3} \\ a_{I6} \\ c_{I1} \\ c_{I2} \end{Bmatrix}, \tag{81}
\end{aligned}$$

where the prescribed uniform and linear voltages $\overline{\Delta\phi}_i$, $\overline{\Delta\phi}_o$, $\overline{\phi}_i$, and $\overline{\phi}_o$ were omitted, as they have already been considered in Problems I and II. Also note that, the system matrices in Eqs. (79) and (80) are identical to those of Problem II in Eqs. (56) and (57), so they need not be recomputed. The sequential solutions of Eqs. (79)–(81) yield the complete set of generalized deformation coordinates ($a_{Ii}, a_{IIi}, a_{IIIi}$, $i = \{3, 6\}$, $c_{Ij}, c_{IIj}, c_{IIIj}$, $j = \{1, 2\}$) of \mathbf{V}_2 .

7.4. Quadratically varying electric displacement on both surfaces

Let the inside and outside lateral surfaces have distinct quadratic voltage distributions along z , given by

$$D_{r_i}(z) = \frac{z^2}{2} \overline{\Delta^2 D}_{r_i} + z \overline{\Delta D}_{r_i} + \overline{D}_{r_i}, \quad D_{r_o}(z) = \frac{z^2}{2} \overline{\Delta^2 D}_{r_o} + z \overline{\Delta D}_{r_o} + \overline{D}_{r_o}. \tag{82}$$

Similar to the discussion in the preceding section, application of the boundary conditions via two differentiations of Eq. (63) and the rearrangement of these results together with Eqs. (71), (73) and (74) give

$$\begin{bmatrix} \kappa_{133} & \kappa_{136} & P_{1E1} & P_{1E2} \\ \kappa_{136} & \kappa_{166} & M_{1E1} & M_{1E2} \\ D_{13r}(r_i) & D_{16r}(r_i) & D_{1E1r}(r_i) & D_{1E2r}(r_i) \\ D_{13r}(r_o) & D_{16r}(r_o) & D_{1E1r}(r_o) & D_{1E2r}(r_o) \end{bmatrix} \begin{Bmatrix} a_{I3} \\ a_{I6} \\ c_{I1} \\ c_{I2} \end{Bmatrix} = \begin{Bmatrix} -(P_{IIP1} + P_{z2}) \\ -(M_{IIP1} + M_{z2}) \\ 2\overline{\Delta^2 D}_{r_i} - D_{IIP1r}(r_i) \\ 2\overline{\Delta^2 D}_{r_o} - D_{IIP1r}(r_o) \end{Bmatrix}, \tag{83}$$

$$\begin{aligned}
& \begin{bmatrix} \kappa_{133} & \kappa_{136} & P_{1E1} & P_{1E2} \\ \kappa_{136} & \kappa_{166} & M_{1E1} & M_{1E2} \\ D_{13r}(r_i) & D_{16r}(r_i) & D_{1E1r}(r_i) & D_{1E2r}(r_i) \\ D_{13r}(r_o) & D_{16r}(r_o) & D_{1E1r}(r_o) & D_{1E2r}(r_o) \end{bmatrix} \begin{Bmatrix} a_{II3} \\ a_{II6} \\ c_{II1} \\ c_{II2} \end{Bmatrix} \\
&= - \begin{Bmatrix} P_{IIP2} \\ M_{IIP2} \\ D_{IIP2r}(r_i) \\ D_{IIP2r}(r_o) \end{Bmatrix} - \begin{bmatrix} \kappa_{II33} & \kappa_{II36} & P_{IIE1} & P_{IIE2} \\ \kappa_{II36} & \kappa_{II66} & M_{IIE1} & M_{IIE2} \\ D_{II3r}(r_i) & D_{II6r}(r_i) & D_{IIE1r}(r_i) & D_{IIE2r}(r_i) \\ D_{II3r}(r_o) & D_{II6r}(r_o) & D_{IIE1r}(r_o) & D_{IIE2r}(r_o) \end{bmatrix} \begin{Bmatrix} a_{I3} \\ a_{I6} \\ c_{I1} \\ c_{I2} \end{Bmatrix}, \tag{84}
\end{aligned}$$

$$\begin{aligned}
& \begin{bmatrix} \kappa_{133} & \kappa_{136} & P_{1E1} & P_{1E2} \\ \kappa_{136} & \kappa_{166} & M_{1E1} & M_{1E2} \\ D_{13r}(r_i) & D_{16r}(r_i) & D_{1E1r}(r_i) & D_{1E2r}(r_i) \\ D_{13r}(r_o) & D_{16r}(r_o) & D_{1E1r}(r_o) & D_{1E2r}(r_o) \end{bmatrix} \begin{Bmatrix} a_{III3} \\ a_{III6} \\ c_{III1} \\ c_{III2} \end{Bmatrix} \\
& = - \begin{Bmatrix} P_{IIIP3} \\ M_{IIIP3} \\ D_{IIIP3r}(r_i) \\ D_{IIIP3r}(r_o) \end{Bmatrix} - \begin{bmatrix} \kappa_{II33} & \kappa_{II36} & P_{IIIE1} & P_{IIIE2} \\ \kappa_{II36} & \kappa_{II66} & M_{IIIE1} & M_{IIIE2} \\ D_{II3r}(r_i) & D_{II6r}(r_i) & D_{IIIE1r}(r_i) & D_{IIIE2r}(r_i) \\ D_{II3r}(r_o) & D_{II6r}(r_o) & D_{IIIE1r}(r_o) & D_{IIIE2r}(r_o) \end{bmatrix} \begin{Bmatrix} a_{II3} \\ a_{II6} \\ c_{II1} \\ c_{II2} \end{Bmatrix} \\
& - \begin{bmatrix} \kappa_{III33} & \kappa_{III36} & P_{IIIIE1} & P_{IIIIE2} \\ \kappa_{III36} & \kappa_{III66} & M_{IIIIE1} & M_{IIIIE2} \\ D_{III3r}(r_i) & D_{III6r}(r_i) & D_{IIIIE1r}(r_i) & D_{IIIIE2r}(r_i) \\ D_{III3r}(r_o) & D_{III6r}(r_o) & D_{IIIIE1r}(r_o) & D_{IIIIE2r}(r_o) \end{bmatrix} \begin{Bmatrix} a_{I3} \\ a_{I6} \\ c_{I1} \\ c_{I2} \end{Bmatrix}, \tag{85}
\end{aligned}$$

where the prescribed uniform and linear voltages $\overline{\Delta D}_r$, $\overline{\Delta D}_{r_o}$, \overline{D}_r , and \overline{D}_{r_o} were omitted, as they have already been considered in Problems I and II. Also note that, the system matrices in Eqs. (83) and (84) are identical to those of Problem II in Eqs. (59) and (61), so they need not be recomputed. The sequential solutions of Eqs. (83)–(85) yield the complete set of generalized deformation coordinates $(a_{ii}, a_{IIIi}, a_{IIIi}, i = \{3, 6\}, c_{Ij}, c_{IIj}, c_{IIIj}, j = \{1, 2\})$ of \mathbf{V}_2 .

7.5. Validation example for problem III

We shall analyze the same homogeneous circular cylinder used for the validation example for Problem II. The cylinder is subjected to linearly varying outside circumferential shear tractions, $\overline{\Delta \sigma}_{\theta o} = 1.0$ Pa/L; linearly varying outside axial shear tractions, $\overline{\Delta \sigma}_{zo} = 1.0$ Pa/L; and a quadratically varying outside surface voltage $\overline{\Delta^2 \phi}_o/2 = 1$ V/L. Thus, the outside voltage is $\bar{\phi}_o = 0$ Volts at $z = 0$, and $\bar{\phi}_o = 400$ Volts at $z = L$. Again, analytical solutions of these problems do not exist. So the semi-analytic results are compared with those obtained via ANSYS (1998). The comparisons of the stresses, displacements and potential through the thickness of the cylinder, normalized with their respective maximum values, are displayed in Fig. 6. The agreement between the two sets of results are quite good. Again note that, these comparisons are made at the mid-length of the cylinder, away from the two ends where the end-effects are observed.

The free-surface integral of the normal electric displacements defined in Eq. (17) yield the values of $\{1.1 \times 10^{-10}, 1.5 \times 10^{-8}, 4.7 \times 10^{-11}, 0.0\}$ Coulombs for the quadratic pressure, quadratic potential, linear axial and linear torsional shear problems, respectively. The corresponding largest individual integrated free-surface fluxes are $\{1.2 \times 10^{-5}, 3.1 \times 10^{-4}, 7.3 \times 10^{-6}, 0.0\}$ Coulombs. Again, the total values are roughly four orders of magnitude smaller than the individual values, thereby validating the consistency of the semi-analytic method.

8. Numerical examples: actuation and sensing with a homogeneous PZT4 cylinder

Here, we first consider the actuation of PZT4 circular cylinders of various geometry and crystal orientations. The cylinders are polarized axially by a unit voltage acting at the clamped end ($z = L$) and grounding at the other end ($z = 0$). As a consequence, the voltages on the interior and exterior surfaces vary linearly between the two extreme values. Fig. 7 displays actuated radial, axial and circumferential displacements per unit length of the cylinder as obtained at the radial coordinate $r/r_i = 1.0$, for different crystal orientation angles $\Theta = [0^\circ, 30^\circ, 60^\circ, 90^\circ]$ and thickness to inner radius ratios $t/r_i = [10, 1.0, 0.1, 0.01]$. The cylinder is not actuated axially or radially for the orientation $\Theta = 90^\circ$, but the same orientation yields

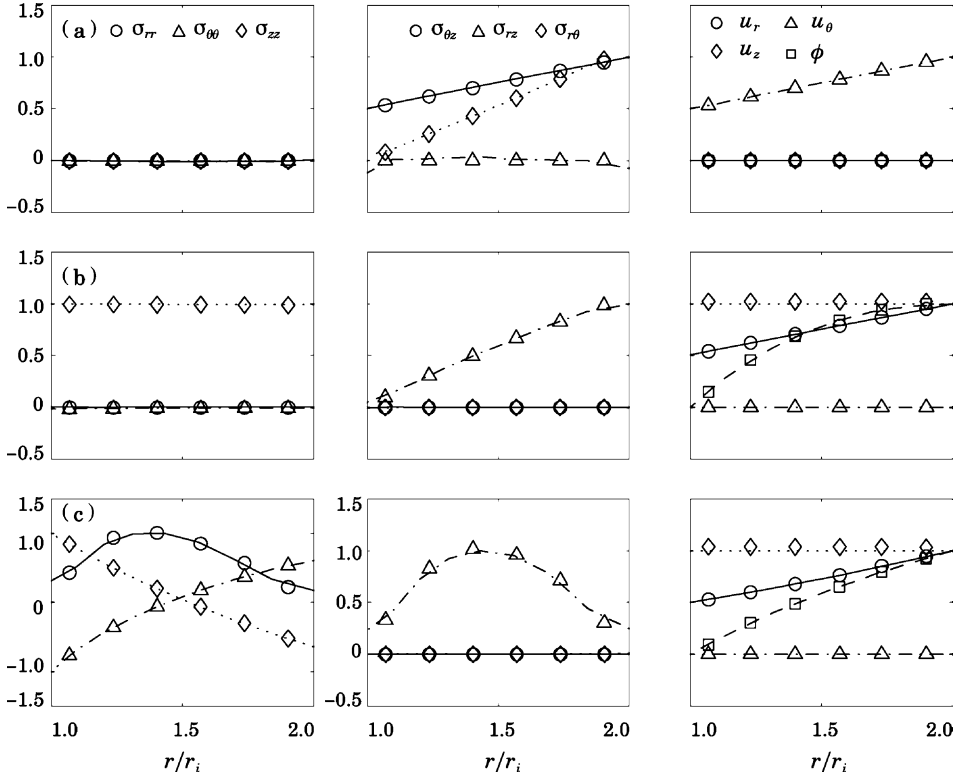


Fig. 6. Validation for Problem III: the results are for linear circumferential (Row a) and axial (Row b) shear tractions, and quadratically varying voltages (Row c) prescribed on the exterior surface of the cylinder. The symbols and the (dashed, dotted, etc.) lines denote the semi-analytic and ANSYS results at the mid-length of the cylinder.

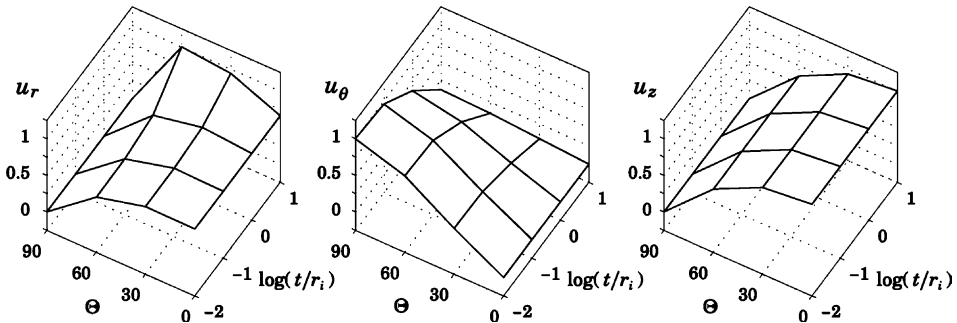


Fig. 7. Actuation example: the variation of radial, rotational and axial displacements (u_r, u_θ, u_z) per unit length of an axially polarized PZT4 circular cylinder depending on the crystal orientation angle (Θ) and the logarithm of the thickness to inner radius ratio (t/r_i). Note that $\Theta = 0^\circ$ corresponds to the properties given in Table 1.

the largest actuation in the circumferential direction. The reverse effect is observed for $\Theta = 0^\circ$. It is also noted that for a radially polarized cylinder, the thickness to radius ratio does not play a significant role in radial and axial actuation, if at all. On the other hand, thin cylinders generally appear to yield a larger circumferential actuation than the thicker ones.

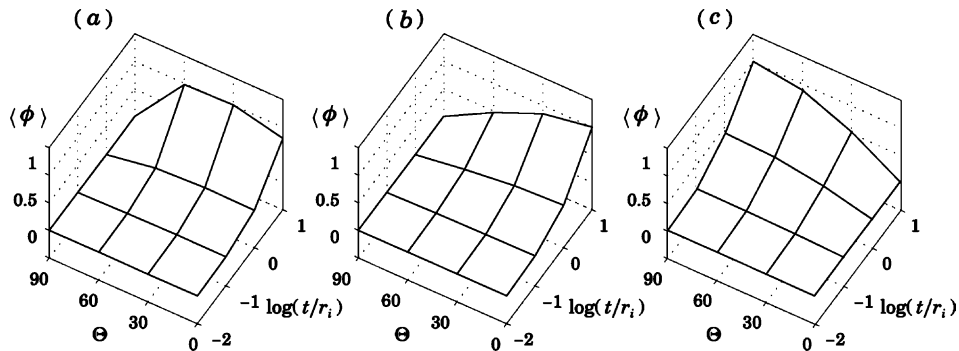


Fig. 8. Sensing example: the variation of electric potential difference between the inside and the outside surfaces $\langle\phi\rangle$ of a PZT4 circular cylinder depending on the crystal orientation angle (Θ) and the logarithm of the thickness to inner radius ratio (t/r_i) under (a) linearly varying pressure, (b) uniform torsional, and (c) uniform axial shear tractions.

The second example involves the sensing of various mechanical surface tractions. Here, we define the difference of inside and outside electric potentials as, $\langle\phi\rangle = |\phi_i - \phi_o|$. In all the problems analyzed, this quantity is uniform along the axial direction and its magnitude can be measured to quantify the surface tractions acting on the cylinder. Fig. 8 displays the electric potential differences $\langle\phi\rangle$ between the inside and outside surfaces for three different loading cases: (a) linearly varying pressure and (b) uniform torsional and (c) axial shear tractions, all acting on the outside surface. It is observed that the thin cylinders do not record a significant electric potential difference for any of the three loading cases. It is also observed that for sensing linear pressure, and uniform torsional and axial shears, the optimum crystal angles are 60° , 0° , and 90° , respectively. The fact that these modes of sensing are out-of-phase can be exploited through the use of multilayered systems in order to develop bimodal or trimodal sensors.

9. Conclusions

A semi-analytical finite method has been presented for analysis of laminated piezoelectric circular cylinders under axisymmetric loads. This method relies on finite element discretization over the thickness of the cylinder and analytical determination of the electromechanical fields along the other dimensions. Such an approach provides significant computational savings over fully-discrete numerical methods. The analysis is based on a statement of the form of the kinematic field in the axial direction that is associated with a particular stress and electric displacement state. Three such states were considered, i.e., uniform, linearly varying and quadratically varying in the z -direction. The generalized coordinates for each kinematic field are determined by consideration of the mechanical and electrical loads prescribed on the lateral surface and the ends of the circular cylinder. While each of the states with a particular variation of stress and electric displacement field was treated separately (i.e., uniform, linear, quadratic, etc.), it is noted that the overall response could have been solved in one step, rather than the three contained in this paper. That which was presented here was intended to add more clarity to the total solution procedure. A one-step solution will nevertheless require data from all of the various steps corresponding to each particular variation of the stress and electric displacement. With the details given for these three states, the extensions to higher-order axially varying states are apparent. It follows that, by a proper superposition procedure, it is possible to obtain solutions under arbitrary (axisymmetric) boundary conditions.

Comparison of present results with known analytical solutions and with three-dimensional finite element results ANSYS (1998) affirms the validity of this method of solution. The provided application example illustrates the sensing and activation features in piezoelectric cylinders with circular symmetry.

Since the analysis is predicated on the relaxed formulation of an equivalent Saint-Venant and Almansi-Michell problem for a circular piezoelectric cylinder, arbitrary point-wise specification of the end conditions cannot be accommodated. Rather, only integral conditions are admissible. To treat arbitrary end conditions, a quantitative analysis of Saint-Venant's principle is needed. This subject will be treated in a subsequent study.

References

ANSYS, 1998. Coupled-Field Analysis Guide, 3rd ed. ANSYS Release 5.5, September 1998.

Batra, R.C., Yang, J.S., 1995. Saint-Venant's Principle in linear piezoelectricity. *Journal of Elasticity* 38, 209–218.

Berlincourt, D.A., Curran, D.R., Jaffe, H., 1964. Piezoelectric and piezomagnetic materials and their function in transducers. In: Mason, W.P. (Ed.), *Physical Acoustics: Principles and Methods*. Academic Press, New York, pp. 169–270.

Bisegna, P., 1998. The Saint-Venant problem for monoclinic piezoelectric cylinders. *Zeitschrift Angewandte Mathematik und Mechanik* 78 (3), 147–165.

Davi, F., 1996. Saint-Venant's problem for linear piezoelectric bodies. *Journal of Elasticity* 43, 227–245.

Galic, D., Horgan, C.O., 2002. Internally pressurized radially polarized piezoelectric cylinders. *Journal of Elasticity* 66, 257–272.

Galic, D., Horgan, C.O., 2003. The stress response of radially polarized rotating piezoelectric cylinders. *Journal of Applied Mechanics* 70, 426–435.

Huang, C.H., Dong, S.B., 2001. Analysis of laminated circular cylinders of materials with the most general form of cylindrical anisotropy. I-axially symmetric deformations. *International Journal of Solids and Structures* 38, 6163–6182.

Ieşan, D., 1986. On Saint-Venant's problem. *Archives of Rational Mechanics and Analysis* 91, 363–373.

Ieşan, D., 1987. Plane strain problems in piezoelectricity. *International Journal of Engineering Science* 25, 1511–1523.

Ma, L.F., Chen, Y.H., Zhang, S.Y., 2001. On the explicit formulations of circular tube, bar and shell of cylindrically piezoelectric material under pressuring loading. *International Journal of Engineering Science* 39 (4), 369–385.

Siao, J.C.T., Dong, S.B., Song, J., 1994. Frequency spectra of laminated piezoelectric cylinders. *Journal of Vibration and Acoustics, ASME* 116, 364–370.

Tarn, J.Q., 2002. Exact solution of a piezoelectric circular tube or bar under extension, torsion, pressuring, shearing, uniform electric loading and temperature change. *Proceedings of the Royal Society of London* 458, 2349–2367.

Tiersten, H.F., 1969. *Linear Piezoelectric Plate Vibrations*. Plenum Press, New York.

Ting, T.C.T., 1996. Pressuring, shearing, torsion and extension of a circular tube or bar of a cylindrically anisotropic material. *Proceedings of the Royal Society of London* 452, 2397–2421.

Ting, T.C.T., 1999. New solutions to pressuring, shearing, torsion and extension of a cylindrically anisotropic elastic circular tube or bar. *Proceedings of the Royal Society of London* 455, 3527–3542.